

https://dspace.org/

Patterns of bone induction by coral-derived vs highly sintered crystalline hydroxyapatite constructs

Alkonti, Assaedi Basher Mohamed

2017
https://hdl.handle.net/10539/24897

Downloaded from a DSpace repository. https://dspace.org/



PATTERNS OF BONE INDUCTION BY CORAL-DERIVED *VS* HIGHLY SINTERED CRYSTALLINE HYDROXYAPATITE CONSTRUCTS

Assaedi B Alkonti

Student number: 1298238

A research report submitted to the Faculty of Oral Health Sciences, University of the Witwatersrand, in partial fulfillment of the requirements for the degree of Master of Science in Dentistry.

Supervisor: Prof. Ugo Ripamonti

School of Oral Health Sciences, Faculty of Health Sciences,

University of the Witwatersrand, Johannesburg, South Africa

2017

DECLARATION

I, Assaedi Alkonti declare that this research report is my own work. It is being submitted for an MSc degree in Oral Medicine & Periodontology at the University of the Witwatersrand, Johannesburg. It has not been submitted before for any degree or examination at this or any other University, and all the sources I have used or quoted have been indicated and acknowledged by complete references.

21th November **2017**.

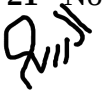

DEDICATION

To my mother, father, beloved wife, precious son and extended family for their support and encouragement.

ABSTRACT

Aim: To evaluate the morphological patterns of bone induction by coral-derived *vs* highly sintered hydroxyapatite constructs.

Methods: Twenty-eight (28) histological slides of harvested tissue samples from the *rectus abdominis* muscle of adult baboons of both coral-derived and highly sintered hydroxyapatite specimens were histologically examined to describe the induction of bone formation along the macroporous spaces of the hydroxyapatite (HA) substrata and the development of osteoblast-like cells within the mesenchymal condensations.

Results: Two specific tissues characterized the tissue invasion within the macroporous spaces of the coral-derived hydroxyapatite constructs, namely, 1: cellular connective tissue matrix penetrated by sprouting capillaries and 2: mesenchymal collagenous condensations that differentiated and attached to the surface of the coral-derived substratum. To the contrary, in the highly sintered constructs, the mesenchymal cellular condensations could not be detected. Fibrovascular tissue was richly invaded by blood vessels almost in direct contact with the sintered hydroxyapatite interface. Elongated spindle-shaped-like cells localised within the mesenchymal collagenous condensation.

The main histological feature that characterised the induction of bone formation by coral-derived hydroxyapatite implant was the induction of mesenchymal collagenous condensation.

In all harvested specimens of highly sintered hydroxyapatite, the initiation of bone formation formed directly against the hydroxyapatite interface without formation of mesenchymal collagenous condensations at the sintered hydroxyapatite interface.

Conclusion: The results obtained from this study further support the concept of construction of solid geometric calcium phosphate osteogenic devices in controlling the induction of bone formation for the treatment of multiple periodontal osseous defects in human patients.

ACKNOWLEDGMENTS

I would like to express my deepest gratitude to my supervisor, Prof. Ugo Ripamonti, who taught and guided me all the way. Thank you for your excellent guidance, caring, patience, monitoring and constant encouragement throughout the learning process – it is much appreciated.

I would also like to thank:

- The staff members of the Oral Medicine & Periodontology Department of the School of Oral Health Science.
- To my family and colleagues who have made this thesis possible and because of whom my postgraduate experience has been one that I will appreciate forever.

Table of Contents

DECLARATION ii
DEDICATION iii
ABSTRACT iv
ACKNOWLEDGMENTS vi
LIST OF FIGURES ix
LIST OF TABLES x
LIST OF ABBREVIATIONS xi
CHAPTER 1- INTRODUCTION & LITERATURE REVIEW 1
1.1. Induction of Bone Formation during Embryonic Development 1
1.1.1. Endochondral bone formation 1
1.1.2. Intramembranous bone formation 3
1.2. Heterotopic Bone Induction 4
1.3. Induction of Bone Formation by Demineralized Bone Matrix (DBM) 6
1.4. Calcium Phosphate Hydroxyapatite and Bone Induction 7
1.5. Intrinsic Induction of Bone Formation 9
1.6. Geometric Induction of Bone Formation 10
1.7. Angiogenesis and the Induction of Bone Formation 11
CHAPTER 2- AIMS AND OBJECTIVES 14
2.1. Aims 14
2.2. Objectives 14
2.3. Rationale of the Study 14
CHAPTER 3- METHODOLOGY 15
3.1. Study Design 15
3.2. Study Sample Size 15
3.3. Data Collection and Analysis 15
3.4. Data Collection Tools 16
CHAPTER 4- RESULTS 19

4.1 Tissue Induction and Morphogenesis by Coral-Derived Macroporous Constructs Implanted in the *Rectus Abdominis* Muscle of *Papio Ursinus* and Harvested on Day 30 19

4.2 Tissue Induction and Morphogenesis by Highly Sintered Macroporous Constructs Implanted in the *Rectus Abdominis* Muscle of *Papio Ursinus* and Harvested on Day 30 20

4.3 Tissue Induction and Morphogenesis by Coral-Derived Macroporous Constructs Implanted in the *Rectus Abdominis* Muscle of *Papio Ursinus* and Harvested on Day 90 21

4.4 Tissue Induction and Morphogenesis by Highly Sintered Macroporous Constructs Implanted in the *Rectus Abdominis* Muscle of *Papio Ursinus* and Harvested on Day 90 22

4.5. Morphological Differences of Patterns of Bone Formation by Coral-Derived *vs* Highly Sintered Crystalline Hydroxyapatite Constructs 23

CHAPTER 5- DISCUSSION 40

CHAPTER 6- CONCLUSIONS 47

REFERENCES 49

APPENDICES 59

Appendix A: Title Approval 59

Appendix B: Ethical Waiver 60

Appendix C: Plagiarism Report 61

LIST OF FIGURES

Figure1 : Olympus Shinjuku, Tokyo Japan light research microscope. 18
Figure2 : Olympus Shinjuku, Tokyo Japan Digital Camera. 18
Figure3 : Peripheral appearance of coral- derived implant on day 30. 26
Figure4 : Tissue invasion within the macroporous spaces of the coral-derived hydroxyapatite constructs on day 30. 27
Figure5 : Hyperchromatic multinucleated giant cells at the surface of coral-derived HA on day 30. 28
Figure6 : Mesenchymal collagenous condensations within concavities of the coral-derived HA substratum and spindle-shaped-like cells on day 30. 29
Figure7 : General appearance of highly sintered HA implant on day 30. 30
Figure8 : Tissue invasion within the macroporus spaces of highly sintered HA and bone differentiation on day 30. 31
Figure9 : Induction of bone formation within the concavity of highly sintered HA substratum (red arrows) on 30 days**.** High power view X175 decalcified section. Modified Goldner's Trichrome stain. 32
Figure10 : Bone differentiation by highly sintered HA interface secreted by osteoblast-like cells on day 30. 33
Figure11 : Compacted collagenous condensations against the coral-derived hydroxyapatite interface on day 90. 34
Figure 12: Group of cells with hyperchromatic nuclei migrated out of the vascular compartment on day 90. High power X300 decalcified section. Toluidine blue stain. 35
Figure13 : Elongated hyperchromatic cells surfacing the newly formed bone at coral- derived HA interface on day 90. 36
Figure14 : Bone formation within the concavities of coral-derived HA spaces with embedded osteocytes on day 90. 37
Figure15 : Extensive bone formation within the concavities of highly sintered HA constructs on day 90 only. 38
Figure 16: Induction of bone formation within the concavity of a sintered hydroxyapatite with osteocytes inside their lacunae on day 90 (black arrows) 150X decalcified section. Modified Goldner's Trichrome stain. 39

LIST OF TABLES

Table 1: Distribution of histological 7 slides according to time period of implantation 16
Table 2: Histological finding of coral-derived and highly sintered HA on day 30 21
Table 3: Histological finding of coral-derived and highly sintered HA on day 90 23
Table 4: Morphological differences of patterns of bone formation by coral-derived vs. highly sintered HA 25

LIST OF ABBREVIATIONS

Ihh: Indian hedgehog.

PTHrP: Parathyroid Hormone-Related Proteins.

ECM: Extracellular Matrix.

VEGF: Vascular Endothelial Growth Factor.

MMP9: Metalloproteinase 9.

BMPs/OPs: Bone Morphogenetic and Osteogenetic Proteins.

CBFA1: Core Binding Factor alpha 1.

TGF-β: Transforming Growth Factor-β.

DBM: Demineralized Bone Matrix.

HA: Hydroxyapatite.

TCP: Tricalcium Phosphate.

BRL: Bone Research Laboratory.

AESC: Animal Ethics Screening Committee.

CHAPTER 1- INTRODUCTION & LITERATURE REVIEW

1.1. Induction of Bone Formation during Embryonic Development

The induction of bone formation starts early during embryonic development by differentiation of mesenchymal cells into bone cells in two ways: firstly, by the formation of a cartilage anlage as in the induction of endochondral bone formation and secondly, by direct cellular condensation with the later intramembranous bone formation as in the induction of the calvaria skeleton (Hall, 1978).

1.1.1. Endochondral bone formation

The induction of endochondral bone formation during embryonic development starts when the mesenchymal outgrowth from the embryo trunk gives rise to the limb buds. The central mesenchymal cells of the limb bud divides rapidly, forming mesenchymal cell condensations. Cells within the central core of mesenchymal condensations differentiate into chondroblasts and chondrocytes forming a cartilage anlage, which acts as a strut upon which the induction of bone formation will develop (Hall, 1978).

Cells at the margins of the cartilage anlage flatten and extend to form thick sheets of connective tissue defined as perichondrium. Chondrocytes in the centre of the cartilage anlage differentiate into hypertrophic chondrocytes (Hall, 1978).

A critical step is the vascular invasion of the mineralized cartilage and of the hypertrophic chondrocytes, which is associated with chondrolysis or death of the cartilage and with mesenchymal cell differentiation into osteoblasts. Osteoblasts in the perichondrium region start secreting bone matrix around the hypertrophic area of cartilage, which is defined as the bone collar (Trueta, 1963).

The induction of a cartilage anlage for the ideal long bone differentiation during embryonic development enhances tri-dimensional growth resulting in development of the cartilaginous growth plate. The cartilaginous growth plate acts as a master for tri-dimensional appositional growth of the mammalian long bones (Ripamonti, 2006).

The development of the growth plate depends on the morphogenesis of the cartilage anlage followed by vascular invasion of the hypertrophic cartilage by blood vessels and sprouting capillaries resulting in the induction of bone formation in angiogenesis (Ripamonti, 2006).

Specific molecular signals regulate endochondral bone formation. Mesenchymal cells within the centre of the condensations start to differentiate initially into chondrocytes which express specific molecular markers such as aggrecan and α 1 (II) collagen (Karsenty and Wagner, 2002).

Expression of such molecular markers enhances chondrocyte proliferation and differentiation into proliferating non-hypertrophic chondrocytes responsible for the cartilage anlage formation. These molecular markers also play a significant role in regulating the rate of cartilage hypertrophy (Karsenty and Wagner, 2002).

Hypertrophic chondrocytes consist of two types of cells. The first group is pre-hypertrophic chondrocytes found under the proliferating chondrocytes, and they are larger than proliferating

chondrocytes. These kinds of cells arrest in growth and continue to express a limited amount of α1 (II) collagen. It mainly expresses the *Indian hedgehog* gene *(Ihh*) which activates the specific molecular factor parathyroid hormone-related proteins (PTHrP) on the surface of hypertrophic chondrocytes. PTHrP enhances the differentiation of these cells into fully differentiated hypertrophic chondrocytes, which is the second group of cells. Fully differentiated hypertrophic chondrocytes do not express α 1 (II) collagen but express α1 (X) collagen (Linsenmayer *et al*., 1991; Poole, 1991; St-Jacques *et al*., 1999; Karsenty and Wagner, 2002).

Before the fully differentiated hypertrophic chondrocytes die by apoptosis, they become surrounded by a calcified cartilage extracellular matrix (ECM). Fully differentiated hypertrophic chondrocytes later express molecular markers such as the vascular endothelial growth factor (VEGF). VEGF stimulates the vascular invasion of the calcified cartilage extracellular matrix by blood vessels followed by chondroclast expression of metalloproteinase 9 (MMP9), which degrades the cartilage (Vu *et al*., 1998; Karsenty and Wagner., 2002).

Cells in contact with the basement membrane of invading capillaries differentiate into osteoblasts secreting the bone extracellular matrix (ECM) rich in type I collagen under the control of bone morphogenetic and osteogenetic proteins (BMPs/OPs) (Paralkar *et al*., 1990).

1.1.2. Intramembranous bone formation

Neural crest-derived mesenchymal cells proliferate to form mesenchymal connective tissue condensations of high cell density. Some of these cells within the mesenchymal condensations

develop into capillaries, and other cells under the control of certain molecular markers alter their shape to become osteoblast-like cells secreting bone matrix which undergo mineralisation to form bone spicules without any cartilage anlage formation (Hall, 1988; Hall & Miyake, 2000).

Some molecular markers of intramembranous bone formation during embryonic development include the bone morphogenetic proteins (BMPs) and an activated transcription factor called core binding factor alpha 1 (CBFA1). BMPs activate the CBFA1 gene in mesenchymal cells to enable it to differentiate directly into osteoblasts secreting bone matrix without the cartilage anlage formation to initiate and form the craniofacial skeleton and calvaria (Hall, 1988).

Extensive research has shown that the process of bone formation by induction in postnatal life recapitulates events which occur in the normal course of embryonic bone development (Wozney, *et al*., 1988; Reddi, 1994; Reddi, 1998). Postnatal bone induction is regulated by the transforming growth factor-β (TGF-β) supergene family (Reddi, 1994; Reddi, 1998; Reddi, 2000; Ripamonti, 2003; Ripamonti, 2006).

1.2. Heterotopic Bone Induction

The heterotopic induction of bone formation is a fascinating phenomenon: cells are induced and transformed into osteoblast-like cells by the osteogenic proteins of the transforming growth factor-β (TGF-β) supergene family (Reddi, 1992; Wozney, 1992; Ripamonti, 2006; Ripamonti, 2003).

The heterotopic induction of bone formation requires three key components (Reddi, 2000): an osteoinductive soluble signal; an insoluble signal or substratum; and responding stem cells.

The osteoinductive soluble signal is a member of the osteogenic proteins of the TGF-β supergene family (Ripamonti, 2003). These osteogenic proteins can initiate bone formation in heterotopic extraskeletal sites of a variety of animal models (Reddi, 1992; Wozney, 1992; Ripamonti, 2006).

The insoluble signal or substratum acts as a delivery system for the osteogenic soluble molecular signals which initiate the induction of the bone formation. The combination of the osteogenic signals with a substratum defines an osteoinductive biomaterial (Sampath & Reddi, 1983; Ripamonti & Reddi, 1995; Reddi, 2000; Ripamonti, *et al*. 2000; Ripamonti, 2009).

Host cells, including undifferentiated mesenchymal cells, start to move toward chemotactic ingredients at the site of heterotopic implantation of the osteoinductive biomaterial. This is followed by proliferation and differentiation of undifferentiated mesenchymal cells into chondrocytes that form a cartilage anlage. The anlage undergoes chondrolysis upon vascular invasion and cartilage death is replaced by bone marrow within the newly formed bone (Reddi, 1981).

Undifferentiated mesenchymal cells can also directly differentiate into osteoblast-like cells forming bone as in intramembranous bone formation by heterotopic implantation of calcium phosphate-based biomaterials in the *rectus abdominis muscle* of adult baboons (*Papio Ursinus)* (Ripamonti, 1990; Ripamonti, 1991).

1.3. Induction of Bone Formation by Demineralized Bone Matrix (DBM)

The classic work of Urist, (1965) Reddi and Huggins, (1972) has described that there are substances capable of inducing heterotopic bone induction after heterotopic implantation of intact demineralized bone matrix (DBM) in extraskeletal sites of different animal models.

Further experimental work has shown that the intact DBM could be dissociatively extracted using chaotropic agents like urea or guanidinium hydrochloride into an inactive insoluble collagenous bone matrix and a soluble protein extract (Sampath and Reddi, 1981; Sampath and Reddi, 1983).

Heterotopic bone formation by induction can only initiate when both the insoluble collagenous bone matrix and the solubilized osteogenic proteins are recombined and later implanted in the rodent subcutaneous site (Sampath and Reddi, 1981; Sampath and Reddi, 1983; Reddi, 2000).

The osteogenic proteins which are delivered by the insoluble collagenous bone matrix and initiate endochondral bone formation are the bone morphogenetic osteogenetic proteins (BMPs/ Ops), members of the TGF-β supergene family (Reddi, 1992; Wozney, 1992; Reddi, 1994; Reddi, 2000; Ripamonti, 2003; Ripamonti, 2004; Ripamonti *et al*., 2004; Ripamonti *et al*., 2005; Ripamonti, 2006).

The molecular and morphological event induced by BMPs/OPs during heterotopic induction of bone formation in the extraskeletal site of animal models recapitulates events that occur during embryonic bone development (Reddi, 1994; Reddi, 1997: Ripamonti, 2003).

1.4. Calcium Phosphate Hydroxyapatite and Bone Induction

Hydroxyapatite (HA) and tricalcium phosphate (TCP) are two types of calcium phosphate-based biomaterials which are chemically similar. HA is a natural inorganic component of bone tissue and several macroporous calcium phosphate-based constructs have been documented to be safe and efficient biomaterials for bone formation (De Groot, 1980; Jarcho, 1981; Jarcho, 1986).

Calcium phosphate biomaterials are highly biocompatible synthetic substrates implanted in hard and soft tissue causing neither tissue toxicity nor inflammatory response. HA has a high affinity for binding BMPs/OPs (Sampath *et al*., 1987; Ripamonti, 1991; Ripamonti, 2006).

The heterotopic induction of bone formation by a variety of calcium phosphate-based biomaterials is a very interesting phenomenon. Osteoinductive biomaterials initiate tissue induction and transformation of osteoblast-like cells secreting bone matrix associated with expression of the selected gene of the transforming growth factor-β (TGF-β) supergene family (Ripamonti, 1991; Ripamonti *et al*, 1999; Ripamonti, *et al*., 2001; Klar *et al*, 2013).

Coral-derived hydroxyapatite is one of the calcium phosphate-based biomaterials of natural origin which is obtained from the hydrothermal exchange of calcium carbonate exoskeleton of marine coral converted into calcium phosphate hydroxyapatite (Roy and Linnehan, 1974).

Highly sintered crystalline hydroxyapatite is one of the synthetic calcium phosphate-based biomaterials prepared when slurry preparations of hydroxyapatite are sintered to form a macroporous construct with specific concavities within the macroporous spaces (Ripamonti *et al*., 1999).

The morphogenesis of bone in porous bioceramics, when implanted in the heterotopic site, was first described when implanting coral-derived hydroxyapatite constructs in *the rectus abdominis* muscle of adult non-human primates (*Papio Ursinus)* (Ripamonti, 1990; Ripamonti, 1991).

The implantation of calcium carbonate coral-derived hydroxyapatite constructs in the *rectus abdominis* muscl*e* of adult baboons shows the differentiation of mesenchymal connective tissue condensations that develop against the macroporous surfaces of the substratum. Such condensations have been shown to differentiate into bone by the differentiation of osteoblast-like cells within the mesenchymal condensations (Ripamonti, 1990; Ripamonti, 1991; Ripamonti, *et al*., 1993).

The development of mesenchymal condensation is a critical phenomenon for the induction of bone formation by coral-derived hydroxyapatite constructs (Ripamonti, 1990; Ripamonti, 1991; Ripamonti *et al*., 1993).

Implantation of coral-derived macroporous hydroxyapatite constructs has led to the manufacture of highly sintered hydroxyapatite constructs (Ripamonti, *et al*., 1999).

The induction of bone formation by coral-derived macroporous constructs occurs between thirty (30) and sixty (60) days of implantation in the muscle of adult baboons (Ripamonti, *et al*., 1993). Similarly, bone formation by highly sintered macroporous construct occurs between thirty (30) and sixty (60) days (Ripamonti, *et al*., 1999).

The induction of bone formation as initiated by such macroporous calcium phosphate-based biomaterials is intramembranous in origin and the induction of cartilage has never been reported (Ripamonti, 1991; Ripamonti *et al*., 1999; Yuan, *et al*., 2002).

1.5. Intrinsic Induction of Bone Formation

The heterotopic implantation of specific types of porous hydroxyapatite biomaterials has led to spontaneous induction of bone formation due to their ability to express BMPs/OPs within concavities of porous hydroxyapatite without exogenous addition of any osteogenic proteins (Ripamonti *et al*., 1993; Ripamont *et al*. 1999).

An ability of some macroporous calcium phosphate-based hydroxyapatite constructs to initiate the intrinsic induction of bone formation is the nano-topographical and geometrical configuration of the substratum (Ripamonti, 1996; Ripamonti *et al*., 1999).

The perfect osteoinductive biomaterials for initiation of bone formation should be biocompatible, carvable and adaptable to different shapes of osseous defects. It should enhance sufficient vascular and connective tissue invasion within the macroporous spaces of substratum in contact with BMPs/OPs (Ripamonti and Duneas, 1996). The calcium phosphate hydroxyapatite biomaterials are considered the most common synthetic biomaterials for bone construction therapy (Jarcho, 1981).

Several studies reported that the particular type of porous hydroxyapatite obtained from the hydrothermal exchange of calcium carbonate exoskeleton of marine coral, converted into calcium phosphate hydroxyapatite, can initiate the induction of bone formation when implanted in the *rectus abdominis* muscle of adult baboons (Ripamonti, 1990; Ripamonti *et al*., 1993; Ripamonti, 1996; van Eeden and Ripamonti, 1994).

1.6. Geometric Induction of Bone Formation

The influence of substratum shape on induction of bone formation was first described by Reddi and Huggins (1973). They found that subcutaneous implantation of two substrata with different geometric configurations blocked the bone induction cascade.

An open-end demineralized root can initiate the induction of bone formation while the substratum with the dead-end tube could not initiate the induction of bone formation but rather initiated the induction of chondrogenesis. They reported that the vascular invasion within the open-end tube was more than that on the dead-end tube which provides more oxygen and nutritional supply which enhances the induction of bone formation (Reddi and Huggins, 1973). Indeed, teeth with the apex intact generate cartilage within the dead-end of the endodontic canal (Reddi and Huggins, 1973).

Many experimental studies have shown the effect of the geometric configuration of demineralized bone matrix (DBM) when implanted in the heterotopic site in the induction of endochondral bone formation, which can be changed by the geometry of the substratum (Reddi, 1974; Sampath and Reddi, 1984).

Coarse powder (420 to 850 μm) of demineralized bone matrix implanted in the subcutaneous space of the rodent, results in induction of endochondral bone formation (Sampath and Reddi, 1984). On the other hand, the implantation of demineralized matrix (fine powder 44 to 74 μm) did not result in the induction of bone formation (Sampath and Reddi, 1984).

The implantation of coral-derived porous hydroxyapatite of both granular and disc configuration in the subcutaneous space of rodents resulted only in the induction of bone formation in porous hydroxyapatites of disc configuration (Sampath and Reddi, 1984).

The addition of exogenous osteogenic protein to porous hydroxyapatite of granular configuration did not result in the induction of bone formation. The above experiments were a clear cut determination of the effect of the geometry on the local induction of bone formation (Sampath and Reddi, 1984; Ripamonti *et al*., 1992).

Intramuscular implantation of highly sintered crystalline hydroxyapatite with repetitive sequences of concavities on both planar surfaces in *Papio Ursinus* was performed to evaluate the geometrical effects of the substratum. This has shown the induction of bone formation within the concavities of the sintered hydroxyapatite construct by day 30 after implantation. This experimental work demonstrates the critical role of the geometry of the substratum in the spontaneous induction of bone formation by controlling the expression of the soluble molecular signals (Ripamonti *et al*., 1999).

1.7. Angiogenesis and the Induction of Bone Formation

Blood vessels are essential for the induction of bone formation (Trueta, 1963). The invading blood vessels and perivascular hyperchromatic stem cells were noted to be within mesenchymal condensations.

Vascular endothelial and pericytic stem cells, together with the basement membrane of invading blood vessels, act as a source of molecular markers that induce and control angiogenesis during osteogenesis (Urist, 1965; Reddi and Huggins, 1972).

Mesenchymal condensations surrounding each central blood vessel in the three-dimensional direction come into close contact with the vascular basement membrane and act as a scaffold for induction of bone formation around the invading vessels. Thus the invading vessels are necessary for the patterning of newly formed bone by the organisation of mesenchymal condensation around it and acted as morphogenetic vessels (Ripamonti *et al*., 2006).

Mesenchymal cells in contact with the basement membrane of invading vessels start differentiating into osteoblast-like cells secreting bone matrix under the control of BMPs/OPs that bind to collagen type IV of the basement membrane of invading blood vessels (Paralkar *et al.*, 1990; Paralkar *et al*., 1991).

The contact between the osteoprogenitors and osteoblast-like cells with vascular invading basement membranes indicates that the specific amino-acid sequences of the basement membrane components, i.e Laminin, are the morphogenetic initiators during the capillary invasion of the ripple-like cascade of bone formation by induction (Vukicevic *et al*., 1990).

1.8. Transforming Growth Factor-β (TGF-β) Supergene Family

The TGF-β supergene family consists of large groups of related proteins that are secreted in the form of a dimer with an active biological form of carboxy-terminal domain consisting of seven cysteine residues (Kingsley, 1994).

Several studies reported that the biologically active TGF-β plays an important role in cell activation, proliferation and differentiation as well as in embryonic tissue morphogenesis, involving osteogenesis, skeletogenesis and cementogenesis (Wozney *et al*, 1988; Reddi, 1994; Ripamonti and Reddi, 1997; Heine *et al*., 1987; Pelton *et al*., 1990; Ripamonti, 2006).

The BMPs/OPs are members of the TGF-β superfamily (Ripamonti, 2003). These osteogenic proteins can initiate bone formation in heterotopic extraskeletal sites of animal models (Reddi, 1992; Wozney, 1992).

Several experimental studies have been performed in an attempt to prove that TGF-β also initiates bone formation. Direct injection of TGF-β1 into the calvarial or overlying the periosteal tissue of the mice and rats resulted in marked increase in bone thickness (Noda and Camilliere, 1989; Marcelli *et al*, 1990; Bolander *et al*., 1991).

The treatment of the cartilage of full thickness rabbit ear wounds by topical application of TGF-β promotes wound healing and bone formation within the cartilage (Beck *et al*., 1991). Heterotopic implantation of recombinant human TGF-β in the *rectus abdominis* muscle of adult baboons induces the induction of endochondral bone formation. This is in marked contrast to any other animal models where the subcutaneous and/or intramuscular implantation of the TGF-β mammalian isoforms do not induce endochondral bone formation (Ripamonti *et al*., 2000; Ripamonti *et al*., 2001).

CHAPTER 2- AIMS AND OBJECTIVES

2.1. Aims

The aim of this study was to evaluate the morphological patterns of bone induction by coral-derived *vs* highly sintered hydroxyapatite constructs.

2.2. Objectives

1. To describe the induction of bone formation along the macroporous spaces of the hydroxyapatite (HA) substratum.
2. To describe the development of osteoblast-like cells within the developing mesenchymal condensations.
3. To see if there are any morphological differences of bone formed by coral-derived *vs* highly sintered hydroxyapatite constructs.

2.3. Rationale of the Study

Are the morphological patterns of bone formation by induction substantially different from coral-derived hydroxyapatite constructs *vs* the highly sintered macroporous crystalline hydroxyapatites?

CHAPTER 3- METHODOLOGY

3.1. Study Design

This study was a descriptive retrospective study. Several histological sections previously prepared for a research study by the Bone Research Laboratory (BRL) of the university were used to compile this retrospective study. All histological sections evaluated were cut from previously embedded specimens of coral-derived and highly sintered hydroxyapatite constructs implanted in the *rectus abdominis* muscle of adult baboons.

3.2. Study Sample Size

Permission to use twenty-eight (28) histological slides of harvested tissue samples from the *rectus abdominis* muscle of adult baboons was obtained from the BRL. All the surgical procedures and tissue harvesting were conducted by Ripamonti. Ethical clearance for the original studies was granted to Ripamonti by the Animal Ethics Screening Committee **(**AESC).

The ethical waiver for this study was granted from the AESC of the University of the Witwatersrand of Johannesburg.

3.3. Data Collection and Analysis

Data was collected from histological examination of twenty-eight (28) histological slides that were previously cut from harvested and processed tissue blocks from the *rectus abdominis* muscle of adult baboons at different time periods, as follows:

Fourteen (14) histological slides of harvested tissue specimens from the *rectus abdominis* muscle of adult baboons on day thirty (30); seven (7) histological slides of coral-derived hydroxyapatite constructs and seven (7) histological slides of highly sintered crystalline hydroxyapatite constructs; Another fourteen (14) histological slides of harvested tissue specimens from the *rectus abdominis* muscle of adult baboons on day (90) of the previously implanted hydroxyapatite biomaterials; seven histological slides of coral-derived hydroxyapatite constructs and seven (7) histological slides of highly sintered crystalline hydroxyapatite constructs (Table 1).

Table 1: Distribution of histological 7 slides according to time period of implantation

28 Histological slides			
14 slides on 30 days of implantation		14 slides on 90 days of implantation	
Seven slides of coral-derived HA	Seven slides of highly sintered HA	Seven slides of coral-derived HA	Seven slides of highly sintered HA

3.4. Data Collection Tools

A Provis AX70 light research microscope (Olympus Shinjuku, Tokyo Japan) was used to examine the histological slides to describe the following:

1. Description of the induction of bone formation along the surface of the hydroxyapatite substrates

2. Description of the formation of connective tissue condensations

3. Description of the development of angiogenesis and vascular invasion within the invading mesenchymal tissue

4. Description of the development of osteoblast-like cells within connective tissue condensations

5. Description of the remodelling of newly formed bone and generation of bone marrow

6. Description of any morphological differences of bone formed by coral-derived hydroxyapatites *vs* highly sintered crystalline hydroxyapatite constructs.

By using a digital camera (Olympus Shinjuku, Tokyo Japan Digital Camera model number C-7070), selected specimens were photographed to report histological patterns of bone formation by induction.



Figure 1: Olympus Shinjuku, Tokyo Japan light research microscope.



Figure 2: Olympus Shinjuku, Tokyo Japan Digital Camera.

CHAPTER 4- RESULTS

4.1 Tissue Induction and Morphogenesis by Coral-Derived Macroporous Constructs Implanted in the *Rectus Abdominis* Muscle of *Papio Ursinus* and Harvested on Day 30

The general appearance of histologically prepared tissue sections when examined under the microscope showed the muscular tissue of the *rectus abdominis* muscle surrounding the implants. Muscle was seen directly attached to the coral hydroxyapatite constructs without fibrous encapsulation. Large blood vessels were shown to surround the implants (Fig. 3).

On day 30, two specific tissues characterized the tissue invasion within the macroporous spaces of the coral-derived hydroxyapatite constructs: 1: cellular connective tissue matrix penetrated by sprouting capillaries; 2: mesenchymal collagenous condensations that differentiated, attached to the coral-derived substratum (Fig. 4).

Hyperchromatic multinucleated giant cells, interpreted as osteoclasts, were seen at the hydroxyapatite interface and also scattered within the fibrovascular tissue which invaded the macroporous spaces of the coral-derived hydroxyapatite construct (Fig. 5).

Mesenchymal connective tissue condensations formed against the hydroxyapatite interface on all specimens harvested on day thirty (30). These were however predominantly shown within the concavities of the substratum (Fig. 6A)

Mesenchymal condensations were organised within the concavities of the hydroxyapatite interfaces at the periphery of the specimens, near the muscular tissue and close to large blood vessels.

Elongated spindle-shaped-like cells were localised within the mesenchymal collagenous condensations arranged parallel to the surface of the hydroxyapatite constructs (Fig. 6B).

Differentiation of bone within the concavities of coral-derived hydroxyapatite specimens could not be detected in any specimen harvested on day 30 (Table 2).

4.2 Tissue Induction and Morphogenesis by Highly Sintered Macroporous Constructs Implanted in the *Rectus Abdominis* Muscle of *Papio Ursinus* and Harvested on Day 30

Histological analysis of tissue specimens of highly sintered crystalline hydroxyapatites on day 30 revealed that the muscle tissue surrounded the implants without fibrous encapsulation. Large blood vessels were seen in close proximity to the substratum (Fig. 7).

The most prominent histological feature was a sustained fibrovascular tissue invasion within the macroporus spaces. Angiogenesis with sprouting capillaries was prominent, in close proximity to the substratum (Figs 8A and 8B).

Mesenchymal cellular condensations could not be detected in any specimen harvested on day 30. Fibrovascular tissue was richly invaded by blood vessels in direct contact with the hydroxyapatite interface (Fig. 8C) Hyperchromatic multinucleated giant cells interpreted as osteoclasts were located along the sintered hydroxyapatite interfaces making resorption lacunae that would initiate the induction of bone formation on day 30. Bone was exclusively

formed within the concavities of the substratum (Fig. 9). In all specimens harvested on day 30, bone formed directly attached to the hydroxyapatite interface (table 2). Bone was lined by a row of hyperchromatic elongated plump cells interpreted as osteoblast-like cells (Fig. 10).

Table 2: Histological finding of coral-derived and highly sintered HA on day 30

Parameters	Coral-derived HA 30 day	Highly sintered HA 30 day
Mesenchymal Condensations	Detected	Undetected
Angiogenesis	Detected	Detected
Osteoclast cells differentiation	Detected	Detected
Induction of bone formation	Undetected	Detected

4.3 Tissue Induction and Morphogenesis by Coral-Derived Macroporous Constructs Implanted in the *Rectus Abdominis* Muscle of *Papio Ursinus* and Harvested on Day 90

Mesenchymal cellular condensations in all specimens harvested on day 90 were more compacted and organised against the hydroxyapatite interface. Condensations surrounded invading blood vessels and capillaries predating the induction of bone formation (Fig. 11A).

Cellular mesenchymal condensations surrounding each central blood vessel were in close contact with the vascular basement membrane of invading capillaries (Fig. 11B).

A group of cells with hyperchromatic nuclei did appear to migrate through the vascular basement membrane into the surrounding fibrovascular tissue (Fig. 12).

Histological analyses of all specimens harvested on day 90 and stained with toluidine blue showed one or two rows of elongated hyperchromatic cells surfacing the newly formed bone within the mesenchymal condensations. These cells were differentiated into osteoblast-like cells in close proximity to invading blood vessels (Fig. 13).

Newly formed bone with embedded osteocytes had differentiated directly within the concavities of the hydroxyapatite, whilst replacing the mesenchymal cellular condensations (Fig. 14).

In many specimens harvested on day 90, bone formed extensively around invading blood vessels and across the macroporous spaces (Table 3).

4.4 Tissue Induction and Morphogenesis by Highly Sintered Macroporous Constructs Implanted in the *Rectus Abdominis* Muscle of *Papio Ursinus* and Harvested on Day 90

Morphological and histological examination of specimens collected on day 90 (see table 3), revealed that bone formed extensively within the concavities and along the macroporous spaces of sintered hydroxyapatite specimens. Osteocytes were embedded within the newly formed bone that had formed in concavities (Figures. 15 &16).

Table 3: Histological finding of coral-derived and highly sintered HA on day 90

Parameters	Coral 90 day	Highly 90 day
Mesenchymal Condensations	Detected	Undetected
Angiogenesis	Detected	Detected
Osteoclast cells	Detected	Detected
Osteoblast –like cells	Detected	Detected
Osteocytes	Detected	Detected
Induction of Bone Formation	Detected	Detected

4.5. Morphological Differences of Patterns of Bone Formation by Coral-Derived *vs* Highly Sintered Crystalline Hydroxyapatite Constructs

The main histological feature that characterised the process of induction of bone formation by coral-derived hydroxyapatite implant is the induction of mesenchymal collagenous condensation along the hydroxyapatite interfaces.

Such condensations play a critical role in bone formation by coral-derived hydroxyapatite where the osteoblast-like cells differentiate within condensations close to the invading blood vessels. Bone formed firstly within mesenchymal condensation at the coral-derived interface.

In all harvested specimens of highly sintered hydroxyapatite, the initiation of bone formation formed directly against the hydroxyapatite interface without formation of mesenchymal collagenous condensations at the hydroxyapatite interface.

Differentiation of bone formation within concavities of coral-derived hydroxyapatite was only detected on day 90, whilst the initiation of bone formation within the concavities of highly sintered hydroxyapatite constructs did differentiate on day 30 after implantation.

Angiogenesis within the macroporous spaces of highly sintered hydroxyapatites appeared more prominent than coral-derived hydroxyapatite constructs.

Osteoclastic resorption of highly sintered hydroxyapatite constructs might have resulted in freeing larger amounts of calcium ions (Ca++), known to recruit angiogenesis (Klar *et al.*, 2013) which was found to be more prominent in highly sintered hydroxyapatite constructs. These might have resulted in more prominent induction of bone formation (Table 4).

Table 4: Morphological differences of patterns of bone formation by coral-derived *vs*. highly sintered HA

Parameters	Coral-derived HA	Highly sintered HA
General appearance	Muscle attached directly to implant without fibrous capsulation	Muscle attached directly to implant without fibrous capsulation
Specific tissues invasion	Cellular connective tissue matrix, sprouting capillaries and mesenchymal collagenous condensations	Blood vessels invasion and sprouting capillaries
Mesenchymal condensation	Compacted and organised mesenchymal cellular condensations predating the induction of bone formation	Absence of mesenchymal cellular condensations. Direct transformation and bone induction at hydroxyapatite interface
Angiogenesis	Less prominent and well differentiated	Substantial angiogenesis and capillary sprouting.
Induction of bone formation	Bone differentiated within mesenchymal cellular condensations on day 90 only	Bone differentiated directly at the hydroxyapatite interface as early as day 30

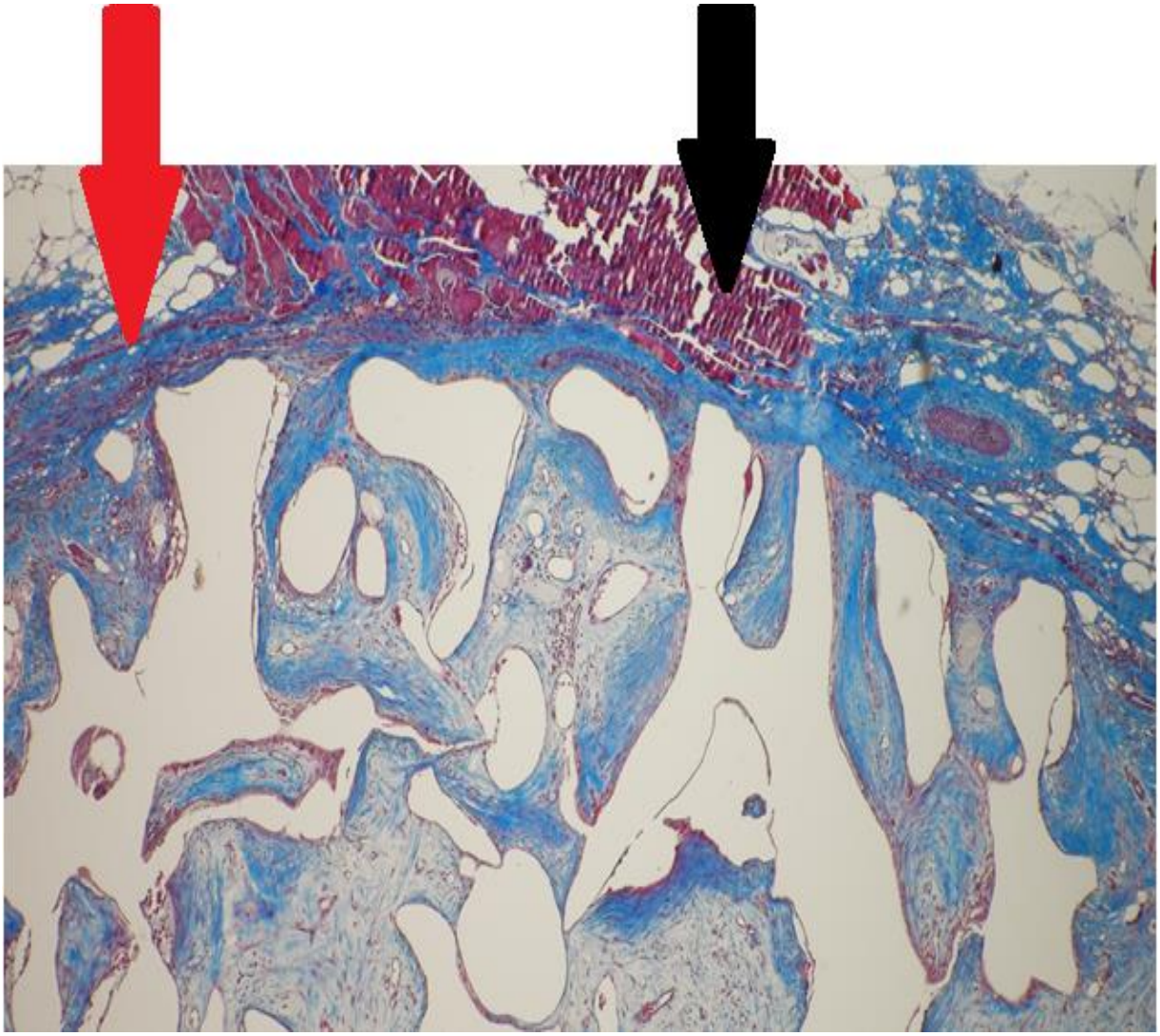

Figure 3: Peripheral appearance of coral- derived implant on day 30.

Photomicrograph showing the muscular tissue at the periphery of coral-derived implant (black arrow). Large blood vessel surrounded the implant (red arrow). 75X decalcified section. Modified Goldner's Trichrome stain.

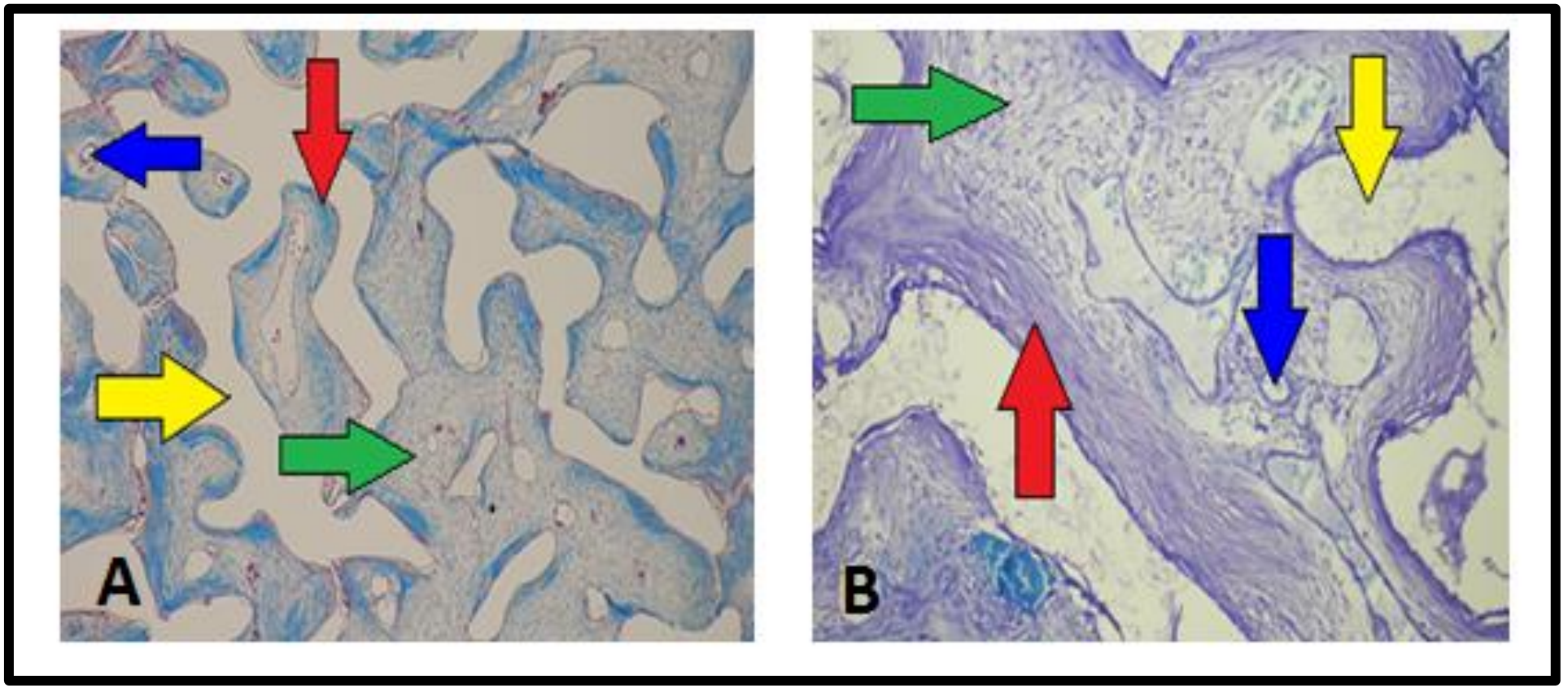

Figure 4: Tissue invasion within the macroporous spaces of the coral-derived hydroxyapatite constructs on day 30.

(A) Low power photomicrograph of tissue patterning initiating the differentiation of mesenchymal condensations at the hydroxyapatite interface (red arrow). Capillary invasion (blue arrow). Cellular connective tissue matrix (Green arrow). Coral-derived hydroxyapatite constructs (yellow arrow). 30X decalcified section. Modified Goldner's Trichrome stain. (B) High power photomicrograph of tissue patterning initiating the differentiation of mesenchymal condensations at the hydroxyapatite interface (red arrow). Capillary invasion (blue arrow). Cellular connective tissue matrix (green arrow).Coral-derived hydroxyapatite constructs (yellow arrow). 150X decalcified section. Toluidine blue stain.

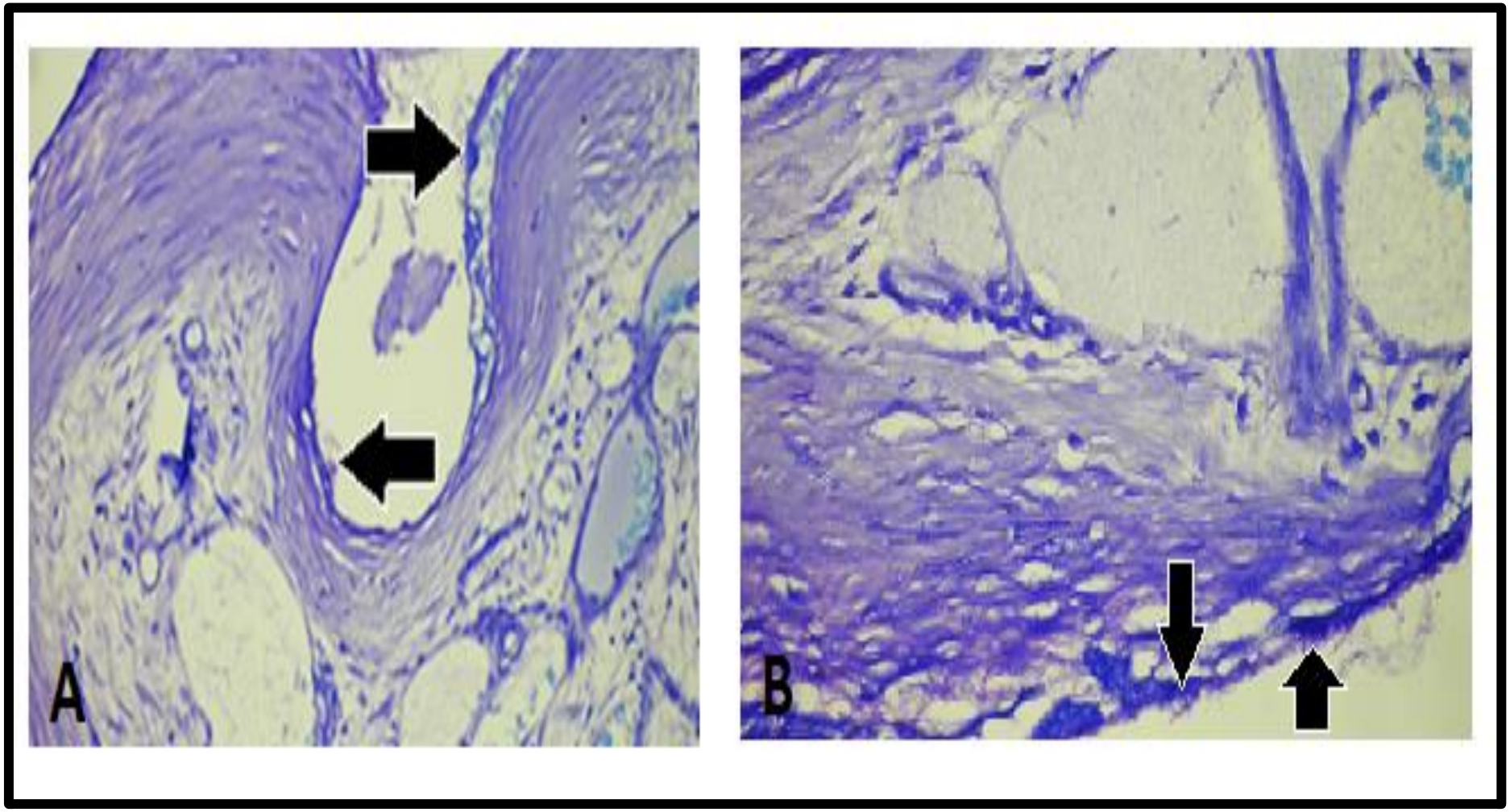

Figure 5: Hyperchromatic multinucleated giant cells at the surface of coral-derived HA on day 30.

(A) Hyperchromatic multinucleated giant cells, interpreted as osteoclasts were located at the hydroxyapatite interface (black arrows). 150X, Toluidine blue. (B) High power photomicrograph of hyperchromatic multinucleated giant cells (osteoclasts) (black arrows). 300X decalcified section. Toluidine blue stain.

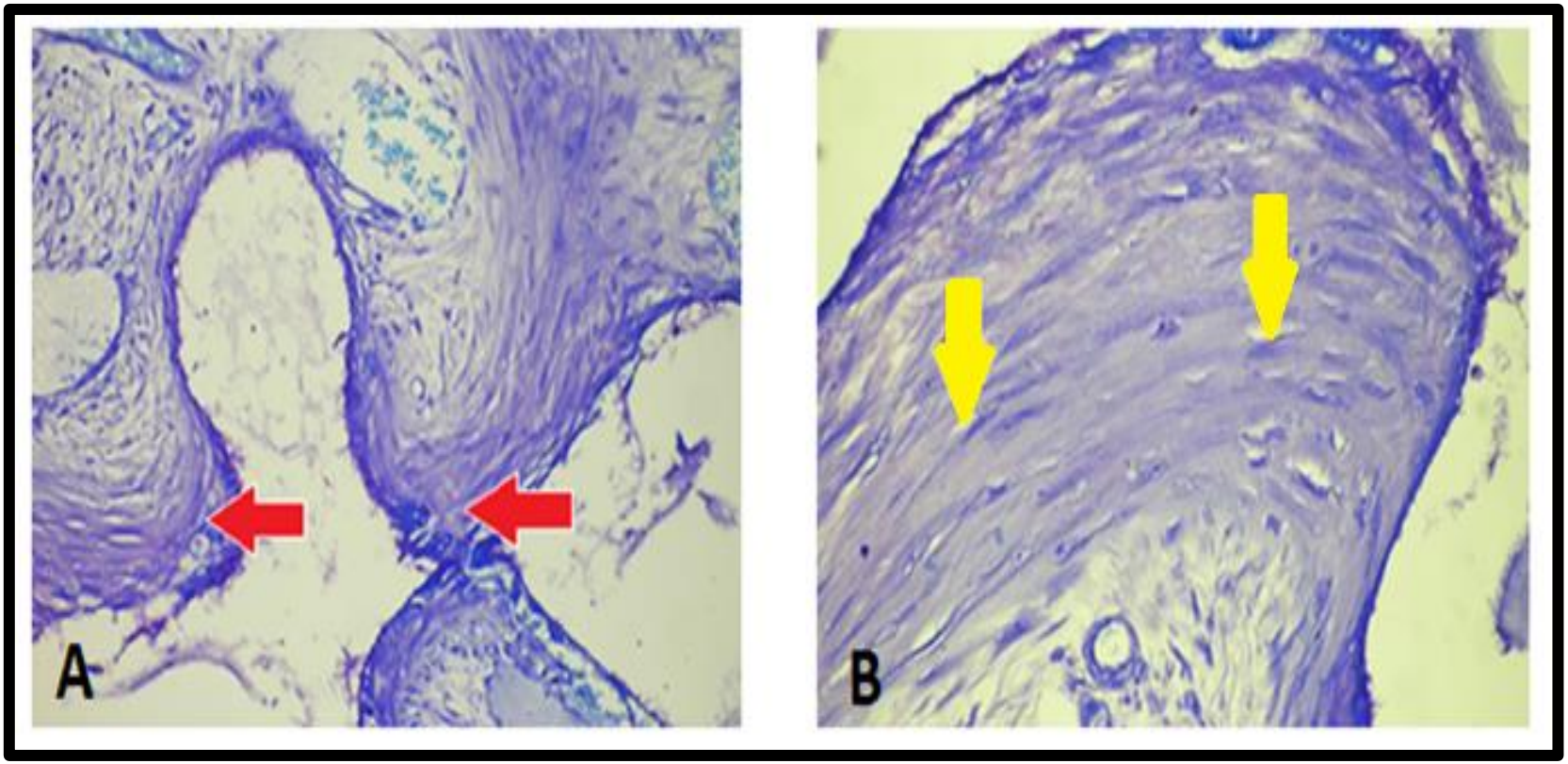

Figure 6: Mesenchymal collagenous condensations within concavities of the coral-derived HA substratum and spindle-shaped-like cells on day 30.

(A) Differentiation of mesenchymal condensations within the concavities of the coral-derived hydroxyapatite substratum (red arrows). 150X, decalcified section Toluidine blue stain.

(B) (B) High power photomicrograph showing elongated spindle-shaped-like cells localised within the mesenchymal collagenous condensation (yellow arrows) 300X, decalcified section. Toluidine blue stain.

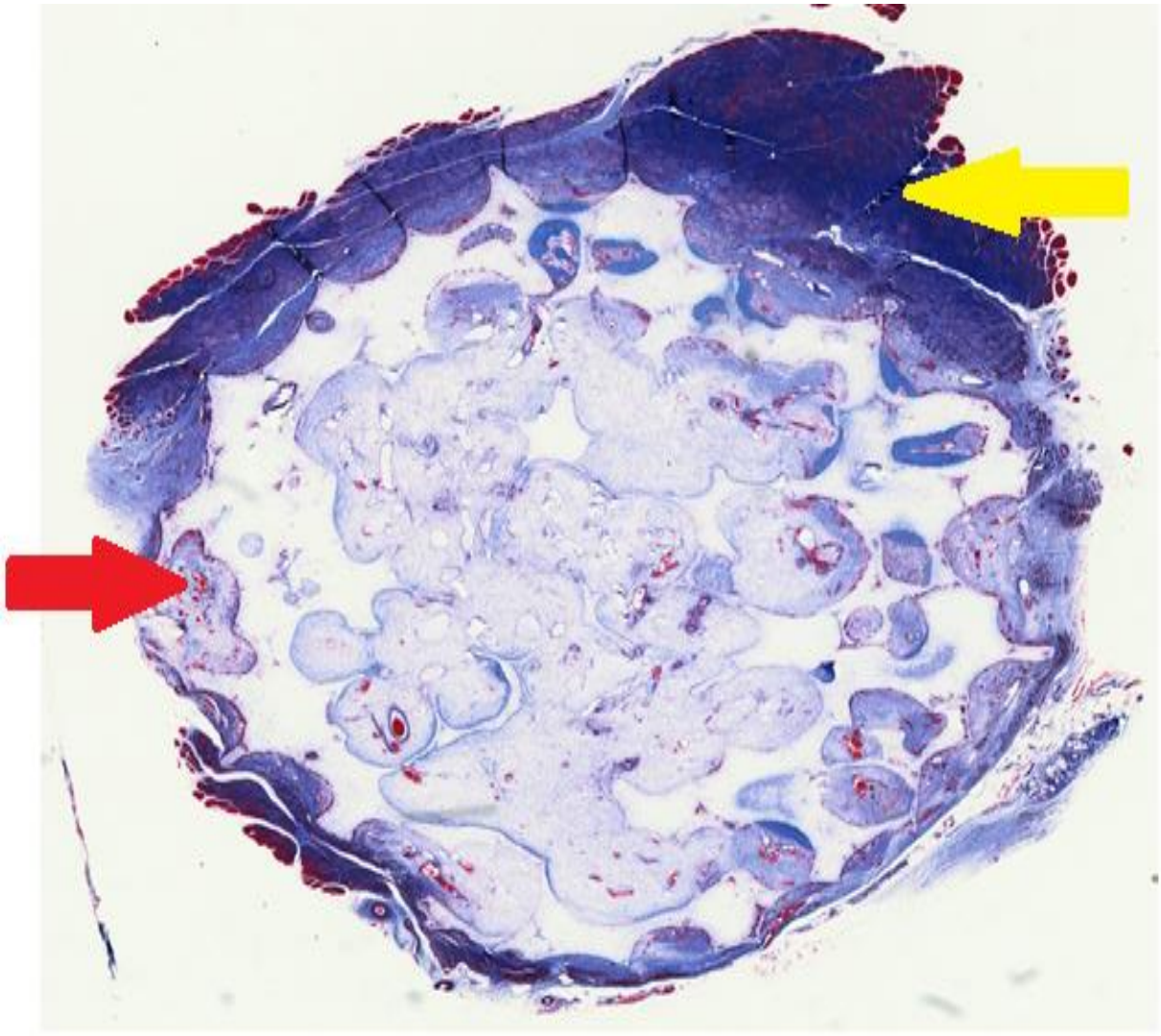

Figure 7: General appearance of highly sintered HA implant on day 30.

Low power photomicrograph showing the muscular tissue at the periphery of highly sintered hydroxyapatite implant (yellow arrow). Large blood vessel surrounded the implant (red arrow) 10X decalcified section. Modified Goldner's Trichrome stain.

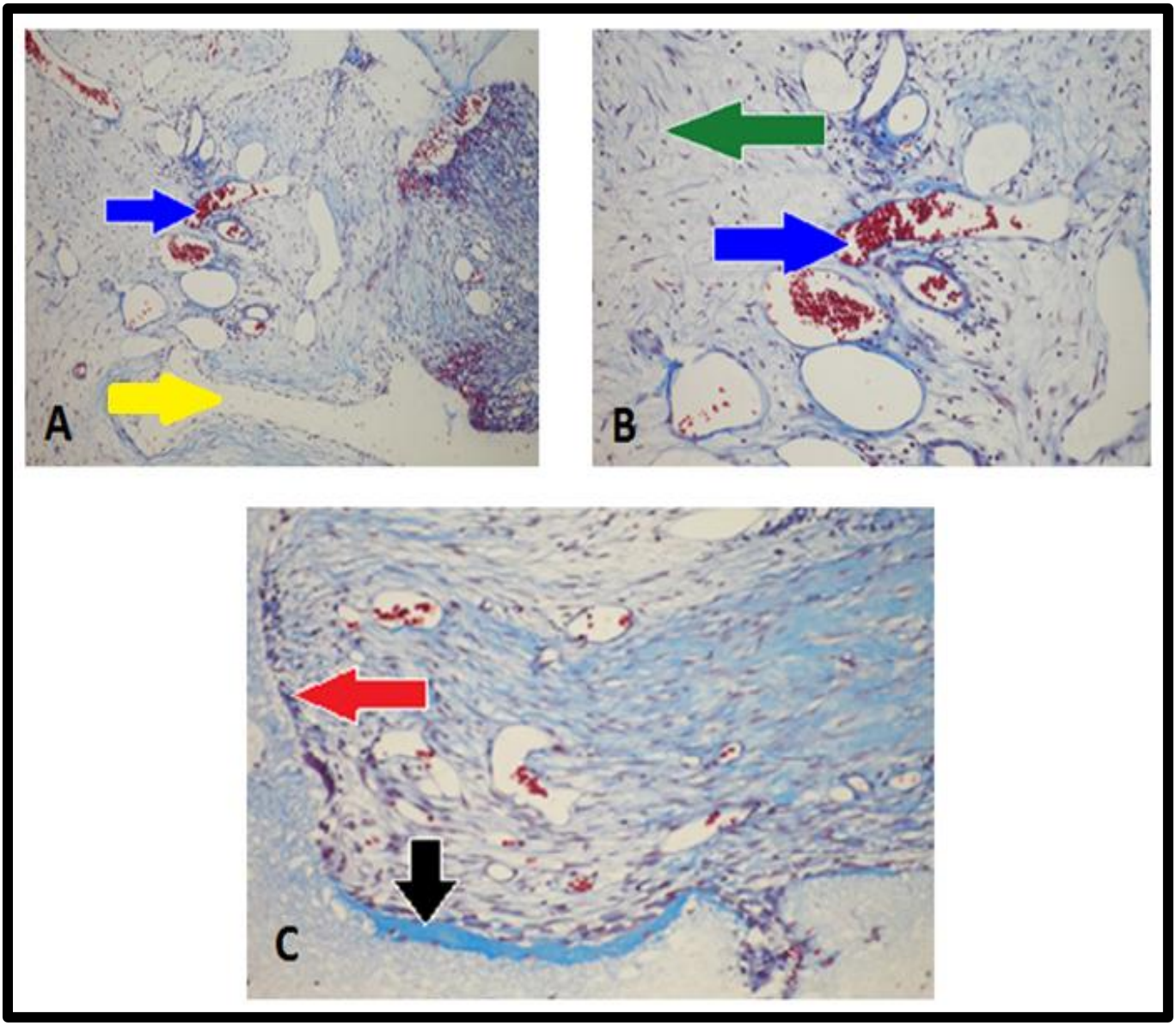

Figure 8: Tissue invasion within the macroporus spaces of highly sintered HA and bone differentiation on day 30.

(A) Highly sintered hydroxyapatite implant (yellow arrow). Angiogenesis with sprouting capillaries (blue arrow).

(B) High power photomicrograph of fibrovascular tissue (Green arrow). Angiogenesis (blue arrow).

(C) High power photomicrograph showing fibrovascular tissue richly invaded by blood vessels in direct contact to the hydroxyapatite interface (red arrow). Newly formed bone directly attached to a concavity of a higly sintered macroporous hydroxyapatite interface (black arrow). 150X decalcified sections. Modified Goldner's Trichrome stain.

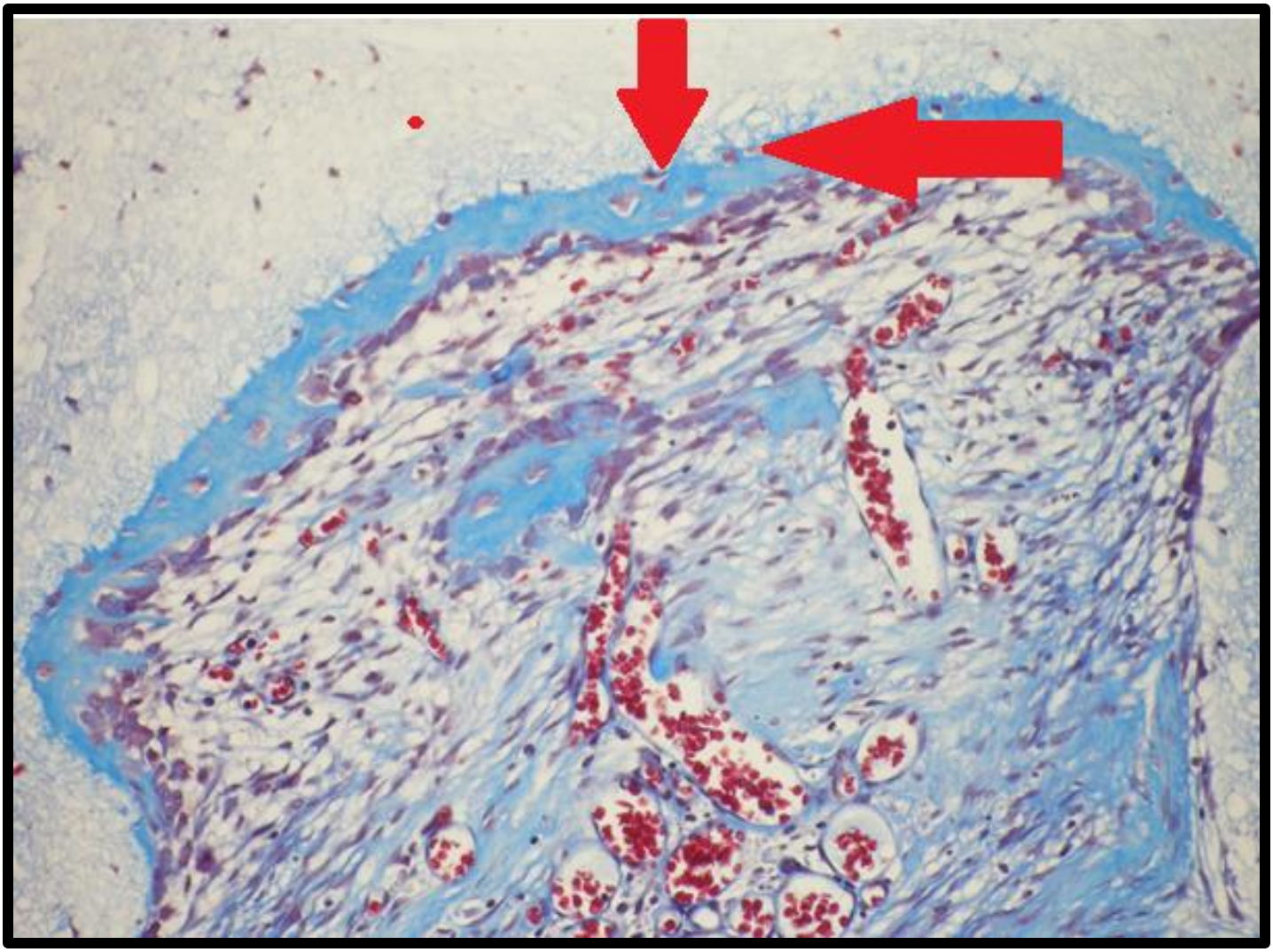

Figure 9: Induction of bone formation within the concavity of highly sintered HA substratum (red arrows) on 30 days**.** High power view X175 decalcified section. Modified Goldner's Trichrome stain.

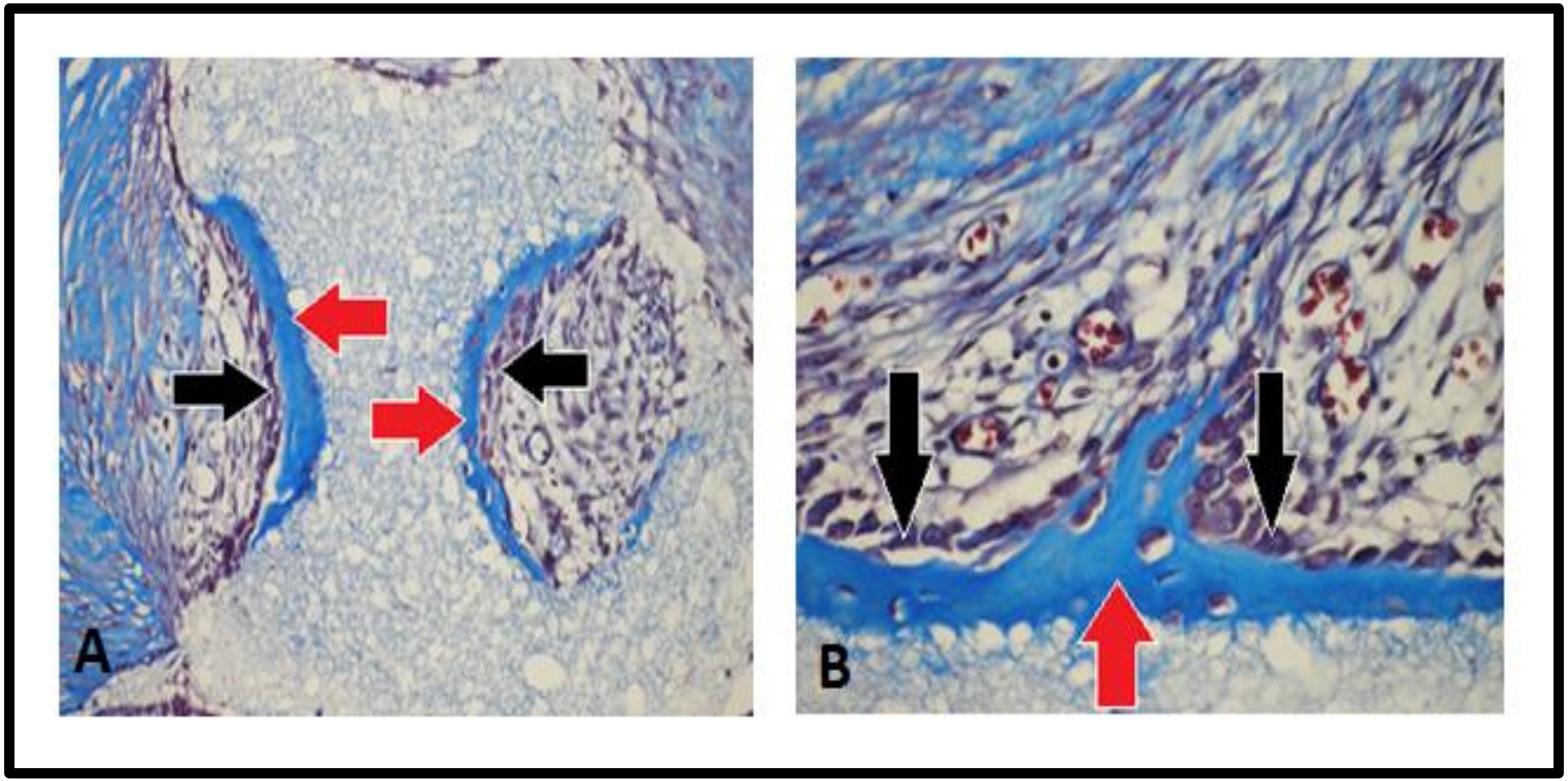

Figure 10: Bone differentiation by highly sintered HA interface secreted by osteoblast-like cells on day 30.

(A) A row of elongated plump cells interpreted as osteoblast-like cells (black arruws). Newly formed bone that initiated within the concavities of the sintered hydroxyapatite substratum (red arrows). 150X decalcified sections. Modified Goldner's Trichrome stain.

(B) High power photomicrograph showing a row of elongated osteoblast-like cells (black arrows). Newly formed bone formed directly and totally hunkering within the highly sintered hydroxyapatite substratum (red arrow). 175X decalcified sections. Modified Goldner's Trichrome stain.

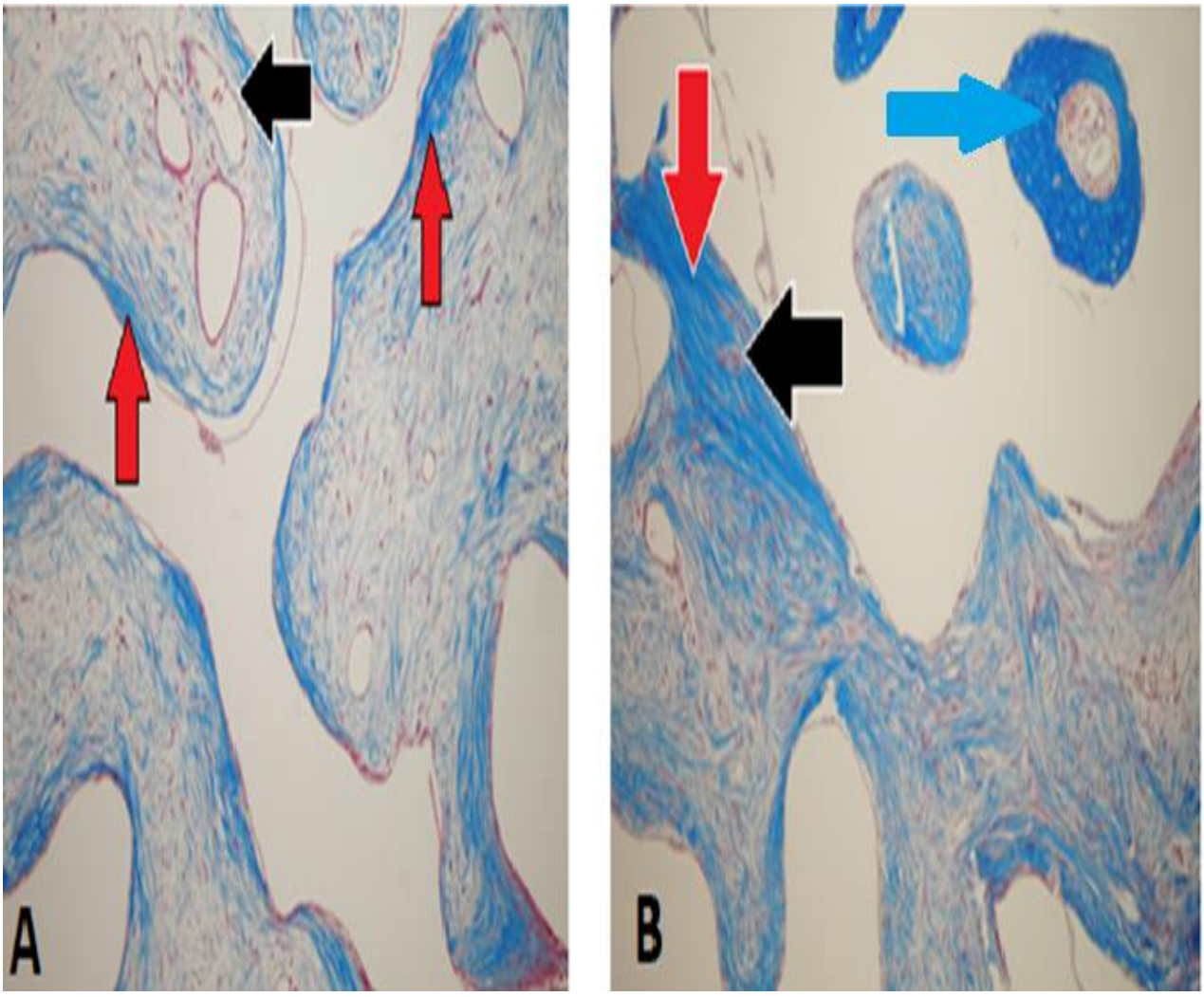

Figure 11: Compacted collagenous condensations against the coral-derived hydroxyapatite interface on day 90.

(A) Compacted and organised mesenchymal collagenous condensations against the hydroxyapatite interface predating the induction of bone formation (red arrows). Invading blood vessel and capillaries surrounded by mesenchymal collagenous condensations (black arrow).

(B) High power photomicrograph showing compacted collagenous condensations (red arrow). Vascular basement membrane in close contact with mesenchymal collagenous condensations (black arrow). Bone formation within compacted condensation around invading blood vessele (blue arrow). X175 decalcified sections. Modified Goldner's Trichrome stain.

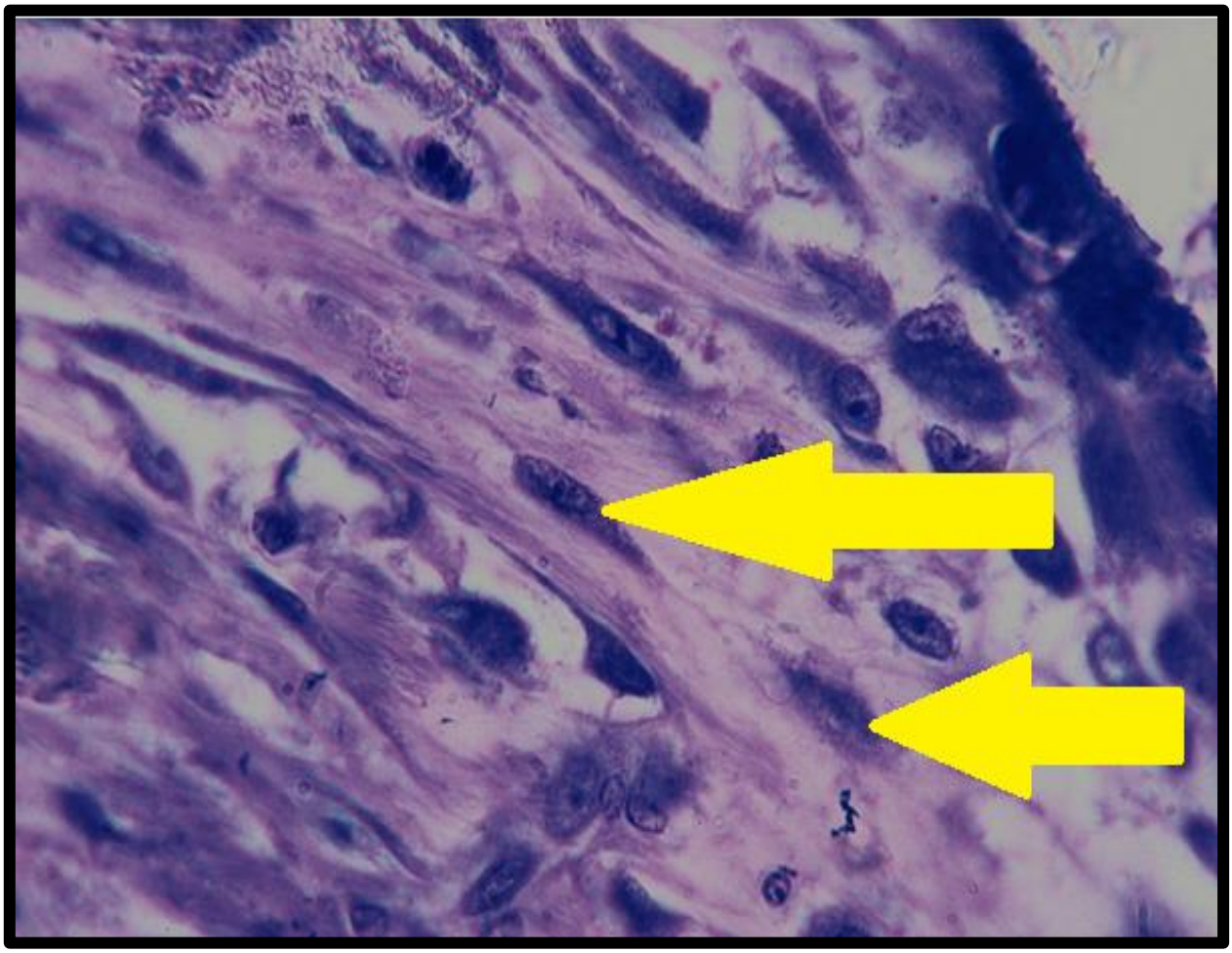

Figure 12: Group of cells with hyperchromatic nuclei migrated out of the vascular compartment on day 90. High power X300 decalcified section. Toluidine blue stain.

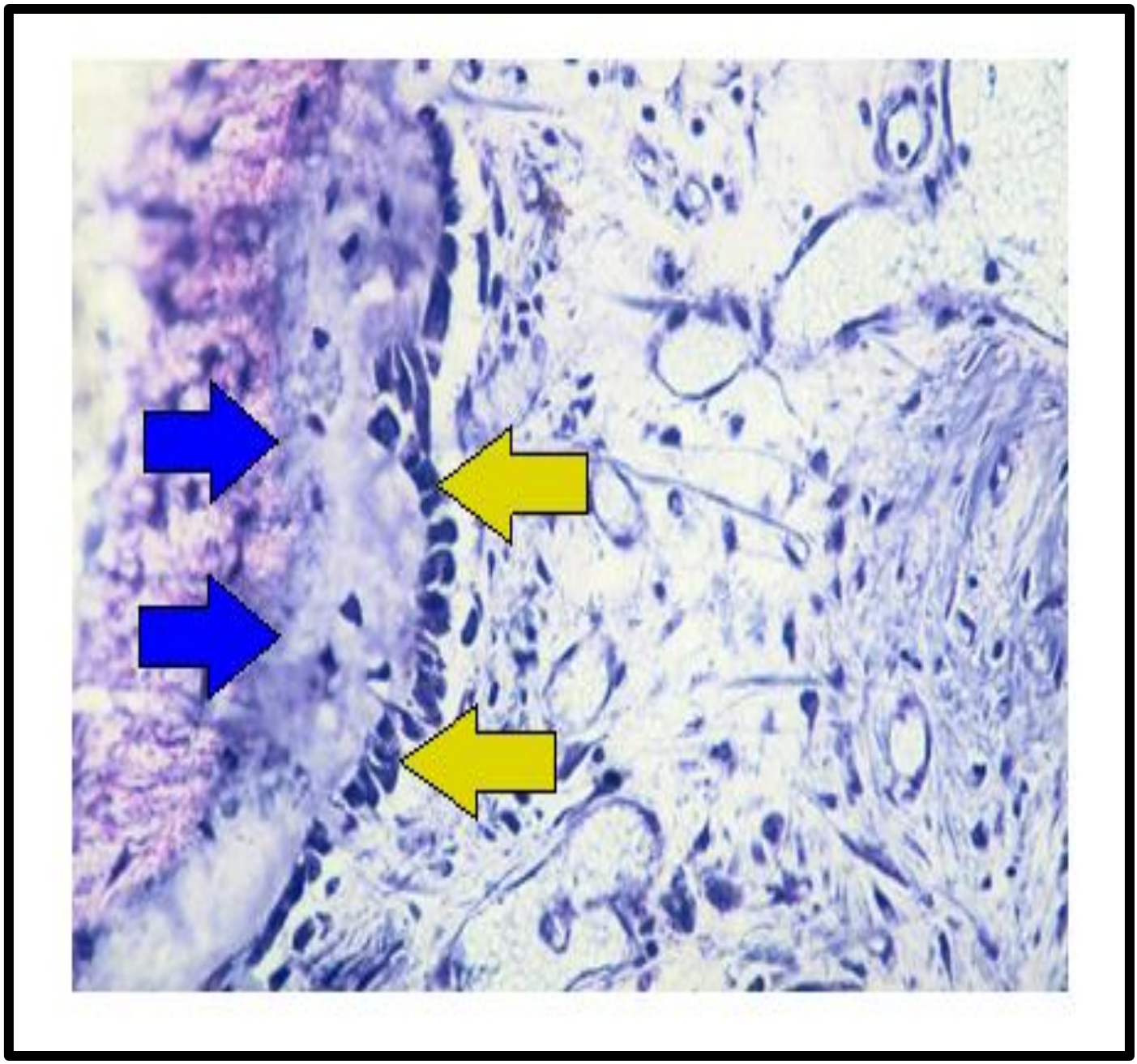

Figure 13: Elongated hyperchromatic cells surfacing the newly formed bone at coral- derived HA interface on day 90.

Blue arrow is newly formed bone attached to the coral-derived HA interface. Yellow arrow is Osteoblast- like cells (Elongated hyperchromatic cells). X175 decalcified section. Toluidine blue stain.

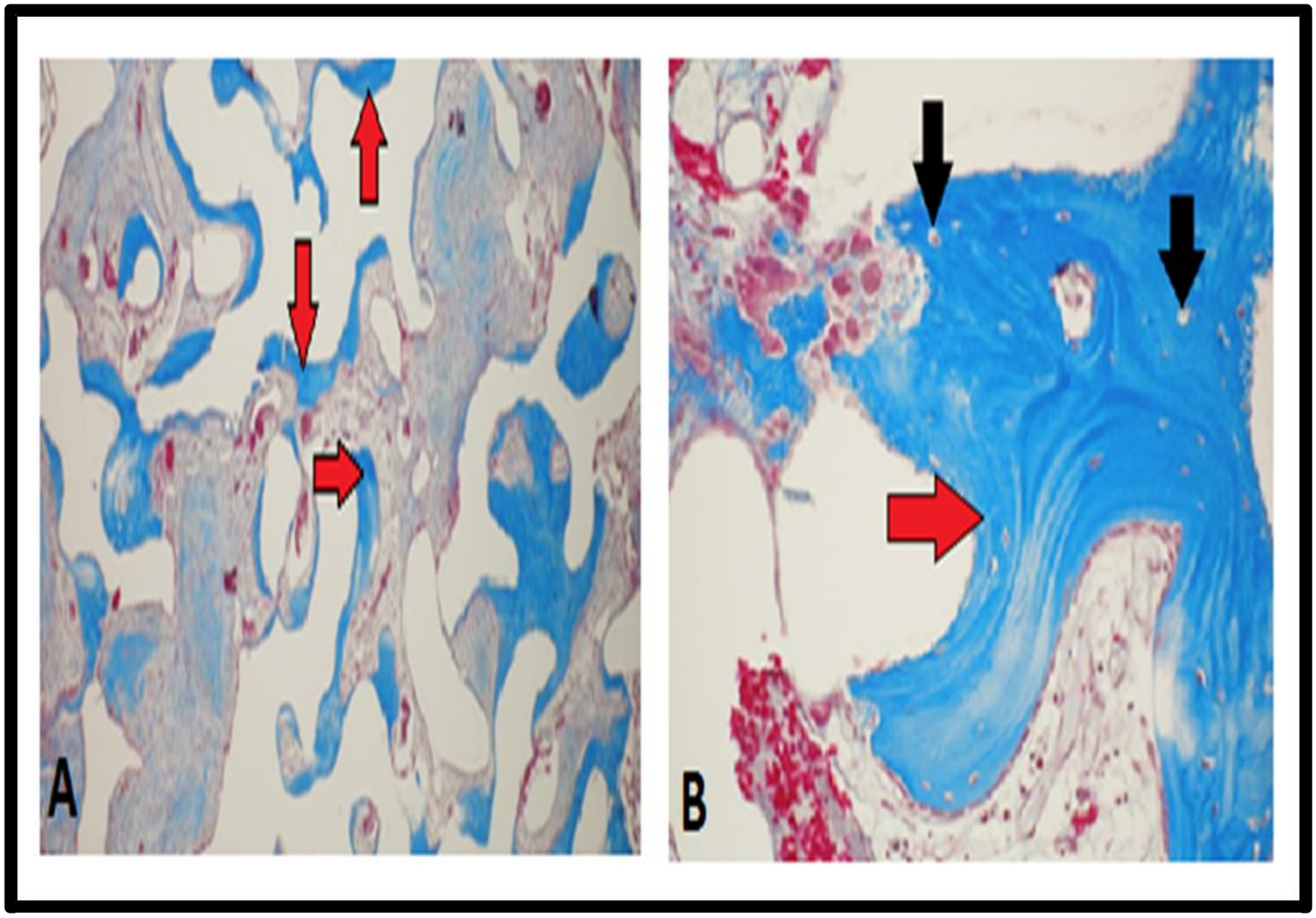

Figure 14: Bone formation within the concavities of coral-derived HA spaces with embedded osteocytes on day 90.

(A) Low power photomicrograph showing bone formation within the concavities of coral-derived hydroxyapatite macroporous spaces (red arrows).). 75X decalcified section. Modified Goldner's Trichrome stain.

(B) High power photomicrograph showing newly formed bone with embedded osteocytes that had differentiated directly within the concavities of the hydroxyapatite substratum (red arrow). Osteocytes inside their lacunae within the formed bone (black arrows). 300X decalcified section. Modified Goldner's Trichrome stain.

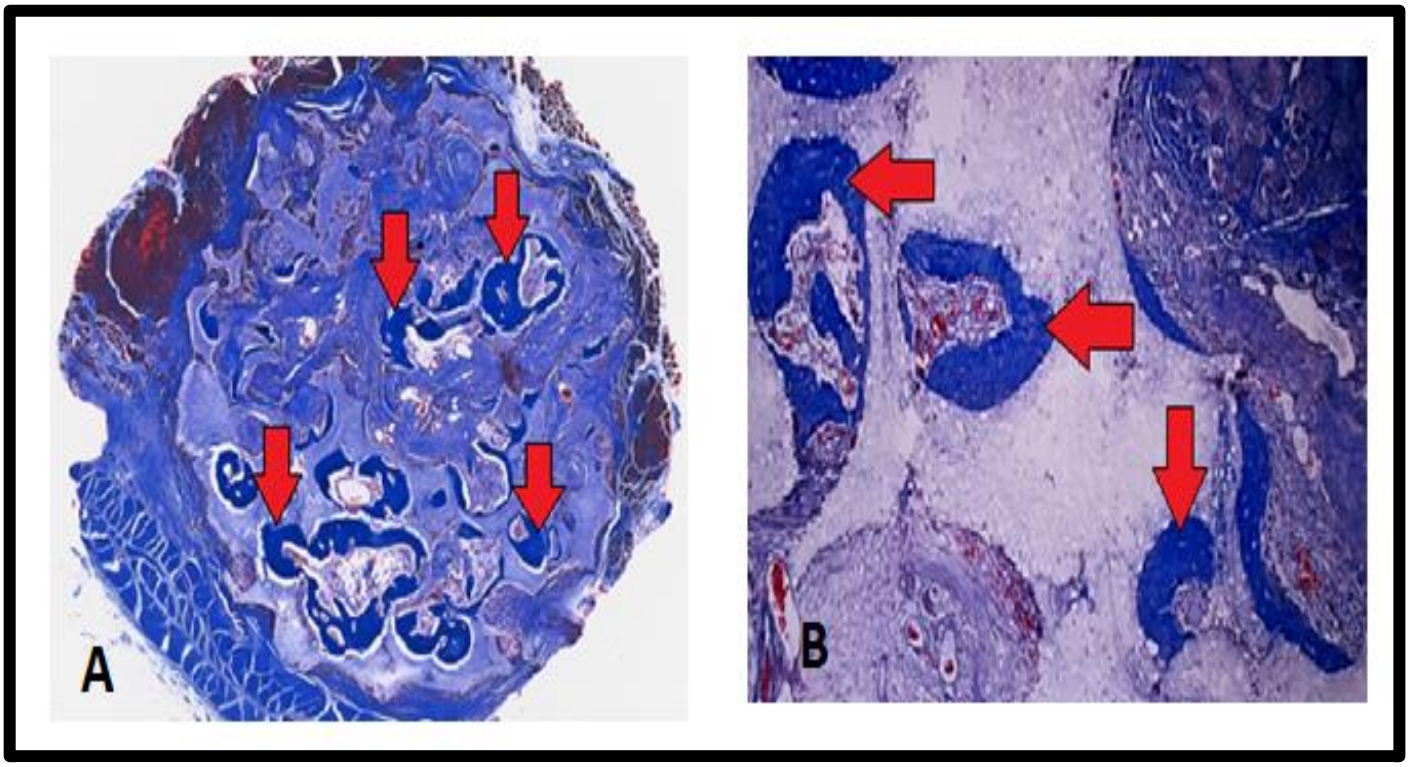

Figure 15: Extensive bone formation within the concavities of highly sintered HA constructs on day 90 only.

Low power photomicrograph showing bone extensively formed within the concavities of the macroporous spaces of sintered hydroxyapatite specimens (red arrows). 10X decalcified section. Modified Goldner's Trichrome stain.

(B) Bone formed only within concavities of a sintered construct (red arrows). 75X decalcified section. Modified Goldner's Trichrome stain.

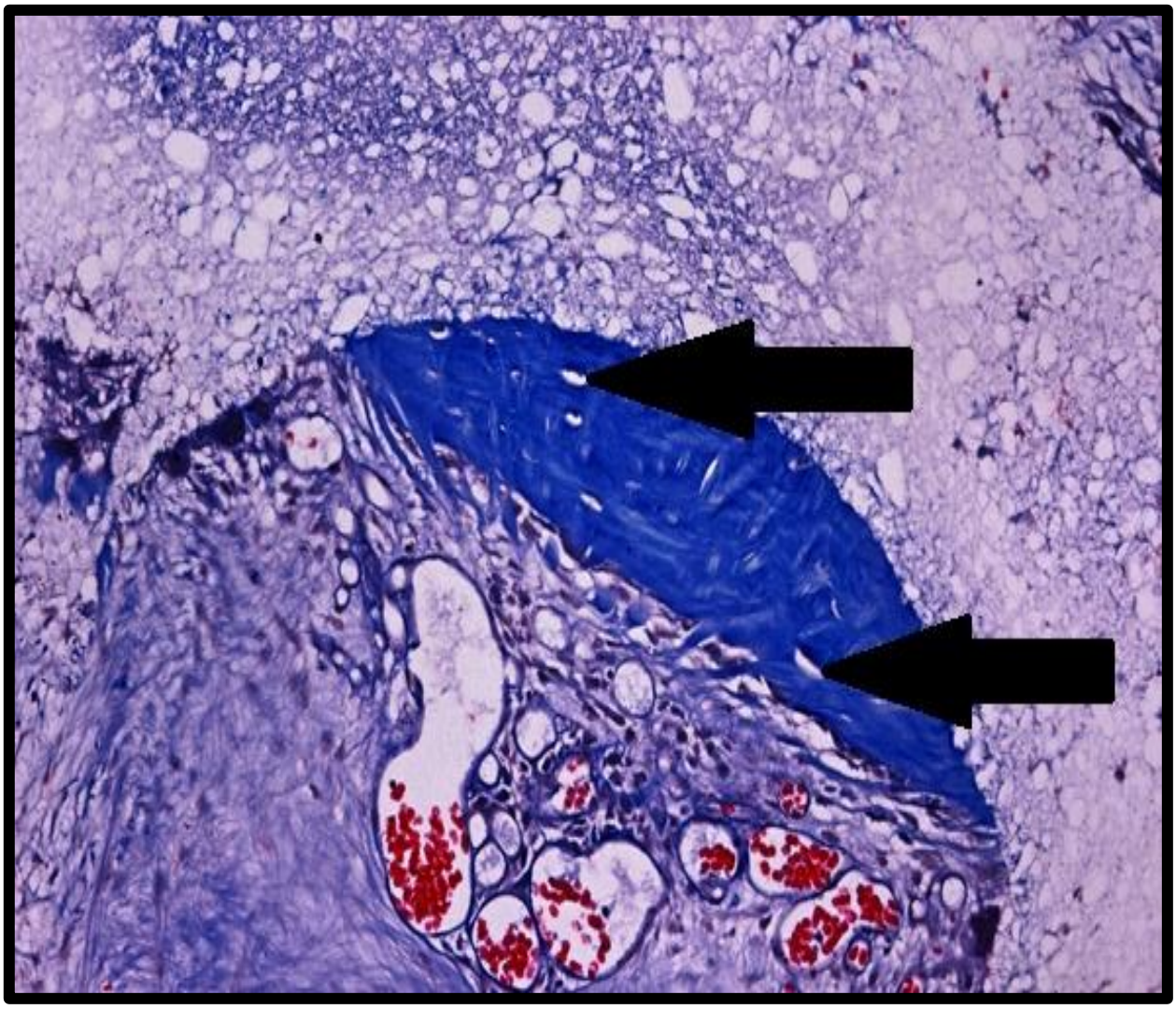

Figure 16: Induction of bone formation within the concavity of a sintered hydroxyapatite with osteocytes inside their lacunae on day 90 (black arrows) 150X decalcified section. Modified Goldner's Trichrome stain.

CHAPTER 5- DISCUSSION

A sound knowledge of the morphological patterns of bone formation by induction using two macroporous hydroxyapatite constructs is necessary to provide information from preclinical studies to clinical contexts, in the treatment of periodontal osseous defects.

Studies have also been done to understand the mechanisms of induction of the spontaneous and intrinsic induction of bone formation by calcium phosphate-based biomaterials (Ripamonti, *et al*. 1993; Ripamonti *et al*., 1999).

The present retrospective study directly compares the induction of bone formation by both coral-derived *vs* highly sintered hydroxyapatite to provide a unique landscape of the induction of bone formation by different calcium phosphate-based constructs.

This study deployed histological sections of previously implanted and harvested tissue specimens from the *rectus abdominis* muscle of several experiments in adult non-human primates (*Papio ursirus).* The study thus provides comprehensive information on the patterns of bone induction by coral-derived *vis-a-vis* highly sintered hydroxyapatite constructs.

The differentiation of mesenchymal collagenous condensations was formed along the surface of the coral-derived hydroxyapatite interface in all specimens harvested on day 30 and 90. The formation of mesenchymal collagenous condensations was only formed within the concavities of the substratum. The collagenous condensation thus was more clearly patterned and organised at the periphery of the harvested specimens.

A thorough examination of such condensation indicated the tight relationship of the substratum geometry with the initiation of the mesenchymal condensation. Concavities act as a nest for cellular adhesion and/or attachment and the mesenchymal condensations were more clearly organised within concavities at the periphery of harvested specimens surrounded by the recipient muscular tissue.

Surrounding blood vessels more appropriately provided responding cells from the vascular and para-vascular environments for migration and attachment to the coral-derived hydroxyapatite constructs.

This interpretation of the available morphological data is in agreement with the study, reporting that the differentiation of mesenchymal collagenous condensations is the earliest morphological event occurring within the macroporous spaces of coral-derived hydroxyapatite constructs (Ripamonti, 1991).

Another study conducted in different animal models (Ripamonti, 1996) revealed that the mesenchymal collagenous condensations at the coral-derived hydroxyapatite interface were always associated with invading blood vessels and sprouting capillaries. This is consistent with the study done by Ripamonti (2006) where the cellular mesenchymal condensations were in close contact with the vascular basement membrane of invading blood vessels and sprouting capillaries. Sprouting capillaries and developing angiogenesis together with mesenchymal condensations are critical morphological events for induction of bone formation (Ripamonti et al., 1993).

Ripamonti suggested that the process of induction of bone formation might have resulted from expression of osteogenic proteins that bind to collagen type IV of the basement membrane of invading blood vessels that initiate the induction of bone formation (Ripamontiet al, .1993).

Binding of bone morphogenic proteins (BMPs) together with angiogenic proteins to type IV collagen of the basement membrane of invading blood vessels is a critical step in the induction of bone formation (Trueta, 1963; Vlodavsky *et al*., 1987; Bolander *et al*., 1988; Paralkar *et al*., 1991).

Present study results are in accordance with previous studies which showed that on day 90 after implantation and before the induction of bone formation, the basement membrane of invading blood vessels was in close proximity to mesenchymal condensations. After the induction of bone formation, the bone forms within the mesenchymal condensations, particularly around invading blood vessels, thus replicating the induction of intramembranous bone formation.

In two studies reported by Ripamonti (1990) and Ripamonti, *et al*. (1993), the differentiation of mesenchymal condensations at the coral-derived hydroxyapatite interface is critical for expression of *bone morphogenic proteins (BMP)* with subsequent induction of bone formation. To unequivocally show bone differentiation in coral-derived macroporous constructs, coral-derived constructs were preloaded with human noggin, a (BMP inhibitor), and implanted in the *rectus abdominis* muscle of adult baboons (Klar *et al*., 2013; Ripamonti *et al*., 2015).

Histological analyses of harvested specimens showed limited and haphazard patterning of mesenchymal condensations along the surface of coral-derived implants referring to the critical correlation between the differentiation of mesenchymal condensations and *BMP* expression (Klar *et al*., 2013; Ripamonti et al., 2015).

In the present study, the differentiation of well organised and compacted mesenchymal collagenous condensations was the first morphological event developing at the coral-derived hydroxyapatite interface on day 30. These were followed by induction of bone formation within the compacted mesenchymal condensations on day 90.

The experimental study conducted by Ripamonti et al., (1993) reported that angiogenesis and invading capillaries within the mesenchymal condensations at the coral-derived hydroxyapatite interface play critical roles in developing osteoblast-like cells within the mesenchymal condensations. Ripamonti et al. (1993) suggested that the differentiation of osteoblast-like cells within mesenchymal condensations might have resulted from the effect of molecular signals expressed within the vascular basement membrane components (Vlodavsky *et al*., 1987; Folkman *et al.,* 1988; Paralkar *et al*., 1991). Such work showed that basement membrane components, in particular type IV collagen, bind both BMPs and angiogenic factors such as the fibroblast growth factor (Vlodavsky *et al*., 1987; Folkman *et al.,* 1988; Paralkar *et al*., 1991).

The present study showed that differentiation of osteoblast-like cells was predominantly confined within the mesenchymal condensations facing the coral-derived hydroxyapatite

interface, close to the invading blood vessels. These findings are in accordance with the results of earlier studies (Ripamonti 1990; Ripamonti 1991; Ripamonti, et al., 1993).

Further experimental studies (Ripamonti et al., 2009) of heterotopic intramuscular implantation of 5% and 13% partially converted hydroxyapatite calcium carbonate constructs in the *rectus abdominis* muscle of adult baboons, indicated that post implantation surface modifications of the substratum by macrophages/osteoclasts play critical roles in differentiation of osteoblast-like cells (Ripamonti, *et al*. 2009). The above was later confirmed by Klar *et al*. (2013). The study evaluated the role of osteoclastogenesis and calcium ions (Ca++) release initiating angiogenesis and osteoblast-like cell differentiation (Klar *et al*., 2013).

Implantation of coral-derived macroporous constructs pre-loaded with the bisphosphonate Zoledronate Zometa (an osteoclast inhibitor) showed a limited bone differentiation highlighting the critical role of osteoclastic activity in modifying the substratum surface topography (Klar *et al*., 2013).

In the present study hyperchromatic multinucleated giant cells (osteoclasts) located at the coral-derived hydroxyapatite interface were also shown to excavate pits and resorption lacunae initiating osteoblast-like cell differentiation. This biomimetizes the remodelling cycle of cortical-cancellous bone where the activated osteoclasts resorb mineralized bone matrix, promoting the osteoblastic differentiation within lacunae excavated by osteoclastic activity (Parfitt et al., 1996).

The induction of bone formation along the surface of highly sintered hydroxyapatite has been evaluated in studies conducted by Ripamonti et al., 1999. The intramuscular implantation of highly sintered hydroxyapatite constructs with repetitive concavities in both planar surfaces in the *rectus abdominis* muscle of adult baboons was regulated by the geometry of the concavities (Ripamonti et al., 1999). The results showed the critical role of geometrical configuration (concavities) in the induction of bone formation.

The present study shows bone differentiation within concavities of the highly sintered hydroxyapatites. Bone formed extensively within the concavities of macroporous spaces of the substratum. Newly formed bone was directly attached to the surface of the highly sintered hydroxyapatite without formation of mesenchymal collagenous condensations as occurred in the induction of bone formation by coral-derived hydroxyapatite constructs.

In this comparative study, the differentiation of angiogenesis within the macroporous spaces of highly sintered hydroxyapatite implants was more prominent than that within the macroporous spaces of coral-derived hydroxyapatite constructs. Also, newly formed bone did differentiate within the highly sintered hydroxyapatite interfaces by day 30 after implantation, earlier than bone forming within coral-derived hydroxyapatite constructs where bone only differentiated on day 90 after implantation. These findings are related to the degree of osteoclastic resorption of highly sintered hydroxyapatite constructs, freeing higher amounts of calcium ions, known to recruit angiogenesis and also more prominent in highly sintered hydroxyapatite constructs. Taken together, the above might have resulted in earlier and more prominent bone formation by highly sintered calcium phosphate constructs.

The results obtained from this study further support the concept of construction of solid macroporous geometric osteogenic devices in controlling the induction of bone formation for the treatment of multiple periodontal osseous defects in human patients.

CHAPTER 6- CONCLUSIONS

The induction of bone formation in postnatal life recapitulates the events that occur in the normal course of embryonic development. Morphogens expressed during embryonic development are re-deployed for postnatal bone regeneration. Both events are equally regulated by selected families of secreted proteins, members of the TGF-β supergene family. Heterotopic implantation of both coral-derived and highly sintered hydroxyapatite constructs in the extraskeletal site of adult baboons initiates the induction of bone formation by expressing and later secreting the osteogenic molecular signals of the TGF-β supergene family. The morphological patterns of bone induction by coral-derived and highly sintered hydroxyapatite are different. The main histological feature that characterised the process of induction of bone formation by coral-derived hydroxyapatite implant is the induction of mesenchymal collagenous condensation along the hydroxyapatite interfaces.

In all harvested specimens of highly sintered hydroxyapatite, the initiation of bone formation was directly formed on the hydroxyapatite interface by secreting differentiated osteoblast-like cells without formation of mesenchymal collagenous condensations at the hydroxyapatite interface.

Differentiation of bone formation within concavities of coral-derived hydroxyapatite was only detected on day 90, whilst the initiation of bone formation within the concavities of the highly sintered hydroxyapatite construct did differentiate on day 30 after implantation.

Angiogenesis within the macroporous spaces of highly sintered hydroxyapatites appeared more prominent than coral-derived hydroxyapatite constructs.

The results obtained from this study further support the concept of construction of solid macroporous geometric calcium phosphate-based osteogenic devices in controlling the induction of bone formation for the treatment of multiple periodontal osseous defects in human patients.

This study provides valuable information in the field of biomaterial sciences with possible translation to periodontal regeneration. Prior knowledge of induction of bone formation by using two calcium phosphate-based biomaterials may help to better understand the mechanisms of the induction of bone formation for the treatment of the periodontal osseous defects. Further studies are required to assess the impact of substratum geometry in the induction of bone formation as well as to compare the morphological patterns of bone formation by highly sintered hydroxyapatite and tri-calcium phosphate biomaterials.

REFERENCES

Beck, L.S., Deguzman, L., Lee, W.P., Xu, Y., McFatridge, L.A. and Amento, E.P., 1991. TGF-β1 accelerates wound healing: reversal of steroid-impaired healing in rats and rabbits. *Growth Factors*, *5*(4), pp.295-304.

Bolander, M.E., Young, M.F., Fisher, L.W., Yamada, Y. and Termine, J.D., 1988. Osteonectin cDNA sequence reveals potential binding regions for calcium and hydroxyapatite and shows homologies with both a basement membrane protein (SPARC) and a serine proteinase inhibitor (ovomucoid). *Proceedings of the National Academy of Sciences*, *85*(9), pp.2919-2923.

De Groot, K., 1980. Bioceramics consisting of calcium phosphate salts. *Biomaterials*, *1*(1), pp.47-50.

Folkman, J., Klagsbrun, M., Sasse, J., Wadzinski, M., Ingber, D. and Vlodavsky, I., 1988. A heparin-binding angiogenic protein-basic fibroblast growth factor-is stored within basement membrane. *The American journal of pathology*, *130*(2), p.393.

Hall, B.K. and Miyake, T., 2000. All for one and one for all: condensations and the initiation of skeletal development. *Bioessays*, *22*(2), pp.138-147.

Hall, B.K., 1978. Types of skeletal tissues. *Developmental and cellular skeletal biology. Academic Press Inc, New York*, pp.1-20.

Hall, B.K., 1988. The embryonic development of bone. *American Scientist*, *76* (2), pp. 174-181.Jarcho, M. 1981. Calcium phosphate ceramics. *Clin. Orthop. 157*: pp.259-278.

Heine, U. I., Munoz, E. F. and Flanders, K. C., *et al*,. 1987. Role of transforming growth factor beta in the development of the mouse embryo. *J Cell Biol. 105*: pp.2861-2876.

Jarcho, M. 1986. Biomaterial aspects of calcium phosphates. Properties and applications. *Dental Clinic North AM, 30*, pp.25-47.

Jarco, M. 1981. Calcium phosphate ceramics as hard tissue prosthetics. Clin. prothop. *Telat. Res, 56*, pp.15-25.

Karsenty, G. and Wagner, E.F., 2002. Reaching a genetic and molecular understanding of skeletal development. *Developmental cell*, *2*(4), pp.389-406.

Kingsley, D.M. 1994. The TGF-beta superfamily: new members, new receptors and new genetic tests of function in different organisms. *Genes Dev*, *8*, pp. 133-146.

Klar, R.M., Duarte, R., Dix-Peek, T., Dickens, C., Ferretti, C. and Ripamonti, U., 2013. Calcium ions and osteoclastogenesis initiate the induction of bone formation by coral-derived macroporous constructs. *Journal of cellular and molecular medicine*, *17*(11), pp.1444-1457.

Linsenmayer, T.F., Chen, Q.A., Gibney, E.I.L.E.E.N., Gordon, M.K., Marchant, J.K., Mayne, R. and Schmid, T.M., 1991. Collagen types IX and X in the developing chick tibiotarsus: analyses of mRNAs and proteins. *Development, 111* (1), pp. 191-196.

Marcelli, C., Yates, A. J. and Mundy, G. R. 1990. *In vivo* effects of human recombinant transforming growth factor beta on bone turnover in normal mice. *J. Bone Miner. Res. 5*: pp.1087-1096.

Noda, M. and Camilliere, J. J. 1989. *In vivo* stimulation of bone formation by transforming growth factor beta. *Endochrinology , 124*: pp.2291-2294.

Paralkar, V.M., Nandedkar, A.K., Pointer, R.H., Kleinman, H.K. and Reddi, A.H., 1990. Interaction of osteogenin, a heparin binding bone morphogenetic protein, with type IV collagen. *Journal of Biological Chemistry*, *265* (28), pp .17281-17284.

Paralkar, V.M., Vukicevic, S. and Reddi, A.H., 1991. Transforming growth factor β type 1 binds to collagen IV of basement membrane matrix: implications for development. *Developmental Biology*, *143* (2), pp. 303-308.

Parfitt, A.M., Mundy, G.R., Roodman, G.D., Hughes, D.E. and Boyce, B.F., 1996. Theoretical perspective: A new model for the regulation of bone resorption, with particular reference to the effects of bisphosphonates. *Journal of Bone and Mineral Research*, *11*(2), pp.150-159.

Pelton, R.W., Hogan, B. L. and Miller, D.A. 1990. Differential expression of genes encoding TGFs β 1,2,3 during murine palatal formation. *Dev. Biol*. *141*, pp. 456-460.

Poole, A.R., 1991. The growth plate: cellular physiology, cartilage assembly and mineralization. *Cartilage: molecular aspects*, pp. 179-211.

Reddi, A. H., 1992. Regulation of cartilage and bone differentiation by bone morphogenetic proteins. *Elsevier Current Trends. 4*(5): pp.850-855.

Reddi, A. H., 2000. Morphogenesis and tissue engineering of bone and cartilage: inductive signals, stem cells, and biomimetic biomaterials. *Tissue Engineering,* 6 (4): pp.351-359.

Reddi, A.H. and Huggins, C., 1972. Biochemical sequences in the transformation of normal fibroblasts in adolescent rats. *Proceedings of the National Academy of Sciences*, USA *69*(6), pp. 1601-1605.

Reddi, A.H. and Huggins, C.B., 1973. Influence of Geometry of Transplanted Tooth and Bone on Transformation of Fibroblasts 1. *Proceedings of the Society for Experimental Biology and Medicine, 143*(3), pp.634-637.

Reddi, A.H., 1974. Bone matrix in the solid state: geometric influence on differentiation of fibroblasts. *Advances in biological and medical physics*, *15*, pp.1-18.

Reddi, A.H., 1981. Cell biology and biochemistry of endochondral bone development. *Collagen and related research*, *1* (2), pp. 209-226.

Reddi, A.H., 1994. Bone and cartilage differentiation. *Current Opinion in Genetics & Development, 4*(5), pp.737-744.

Reddi, A.H., 1997. Bone morphogenetic proteins: an unconventional approach to isolation of first mammalian morphogens. *Cytokine and Growth Factor Reviews, 8* (1), pp. 11-20.

Reddi, A.H., 1998. Role of morphogenetic proteins in skeletal tissue engineering and regeneration. *Nature Biotechnology*, *16* (3), pp. 247-252.

Ripamonti, U. & Reddi, A.H., 1995. Bone Morphogenetic Proteins: Applications in Plastic and Reconstructive Surgery *Adv Plast Reconstr Surg,*11: pp. 47-73.

Ripamonti, U. 1996. Osteoinduction in porous hydroxyapatite implanted in heterotopic sites of different animals models. *Biomaterials*, *17*, pp. 31-35.

Ripamonti, U. and Duneas, N., 1996. Tissue engineering of bone by osteoinductive biomaterials. *MRS Bulletin*, *21*(11), pp.36-39.

Ripamonti, U. and Reddi, A.H., 1997. Tissue engineering, morphogenesis, and regeneration of the periodontal tissues by bone morphogenetic proteins. *Critical Reviews in Oral Biology & Medicine*, *8*(2), pp.154-163.

Ripamonti, U., 1990. Inductive bone matrix and porous hydroxyapatite composites in rodents and nonhuman primates. *In Handbook of Bioactive Ceramics, vol. II: Calcium Phosphate and Hydroxyapatite Ceramics*, pp. 245-253.

Ripamonti, U., 1991. The morphogenesis of bone in replicas of porous hydroxyapatite obtained from conversion of calcium carbonate exoskeleton of coral. *J. Bone Joint Surg. 73-A*, pp. 692-703.

Ripamonti, U., 2003. Osteogenic proteins of the TGF-β Superfamily. *In Encyclopedia of Hormones*, pp. 80-86

Ripamonti, U., 2004. Soluble, insoluble and geometric signals sculpt the architecture of mineralized tissues. *J Cell Mol Med 8*: pp.169-180.

Ripamonti, U., 2006. Soluble osteogenic molecular signals and the induction of bone formation. *Biomaterials, 27,*: pp.807-822.

Ripamonti, U., 2009. Biomimetism, biomimetic matrices and the induction of bone formation. *J Cell Mol Med, 13* (9b), pp.2953-2972.

Ripamonti, U., Crooks, J. & Kirkbride, A.N., 1999. Sintered porous hydroxyapatites with intrinsic osteoinductive activity: geometric induction of bone formation. *South African Journal of Science 95*(8), pp.335.

Ripamonti, U., Crooks, J., Khoali, L. and Roden, L., 2009. The induction of bone formation by coral-derived calcium carbonate/hydroxyapatite constructs. *Biomaterials*, *30*(7), pp.1428-1439.

Ripamonti, U., Crooks, J., Tucker, M.M., Sampath, T.K., Rueger, D.C. and Reddi, A.H., 2000. Long-term evaluation of bone formation by osteogenic protein 1 in the baboon and relative efficacy of Bone-derived Bone morphogenetic proteins delivered by irradiated xenogeneic collagenous matrices. *Journal of Bone and Mineral Research, 15* (9), pp. 1798-1809.

Ripamonti, U., Dix-Peek, T., Parak, R., Milner, B. and Duarte, R., 2015. Profiling bone morphogenetic proteins and transforming growth factor-β s by hTGF-β 3 pre-treated coral-derived macroporous bioreactors: the power of one. *Biomaterials*, *49*, pp.90-102.

Ripamonti, U., Ferretti, C. and Heliotis, M., 2006. Soluble and insoluble signals and the induction of bone formation: molecular therapeutics recapitulating development. *Journal of Anatomy*, *209* (4), pp. 447-468.

Ripamonti, U., Herbst, N.N. and Ramoshebi, L.N., 2005. Bone morphogenetic proteins in craniofacial and periodontal tissue engineering: experimental studies in the non-human primate Papio ursinus. *Cytokine and Growth Factor Reviews*, *16* (3), pp. 357-368.

Ripamonti, U., Ma, S. and Reddi, A.H., 1992. The critical role of geometry of porous hydroxyapatite delivery system in induction of bone by osteogenin, a bone morphogenetic protein. *Matrix*, *12*(3), pp.202-212.

Ripamonti, U., Nathaniel Ramoshebi, L., Patton, J., Teare, J., Matsaba, T. and Renton, L., 2004. Sculpturing the architecture of mineralized tissues: Tissue engineering of bone from soluble signals to smart biomimetic matrices. *Pharmaceutical biotechnology: Drug discovery and clinical applications*, pp. 281-297.

Ripamonti, U., Ramoshebi, L.N., Matsaba, T., Tasker, J., Crooks, J. and Teare, J., 2001. Bone induction by BMPs/OPs and related family members in primates. *J Bone Joint Surg Am*, *83*(1 suppl 2), pp.S116-S127.

Ripamonti, U., Van den Heever, B. & Van Wyk, J., 1993. Expression of the Osteogenic Phenotype in Porous Hydroxyapatite Implanted Extraskeletally in Baboons. *Matrix, 13*(6) pp. 491-502.

Roy, D. M. & Linnehan, S. K., 1974. Hydroxyapatite formed from coral skeletal carbonate by hydrothermal exchange. *Nature, 247* (5438), pp.220-222.

Sampath, T. and Reddi, A., 1983. Homology of bone-inductive proteins from human, monkey, bovine, and rat extracellular matrix. *Proceedings of the National Academy of Sciences*, 80 (21), pp. 6591-6595.

Sampath, T.K. and Reddi, A.H., 1981. Dissociative extraction and reconstitution of extracellular matrix components involved in local bone differentiation. *Proceedings of the National Academy of Sciences*, *78* (12), pp.7599-7603.

Sampath, T. and Reddi, A. 1984. Importance of geometry of the extracellular matrix in endochondral bone differentiation. *The Journal of cell biology*, *98*(6), pp.2192-2197.

Sampath, T. K., Muthukumaran, N. and Reddi, A.H., 1987. Isolation of osteogenin, an extracellular matrix-associated, bone-inductive protein, by heparin affinity chromatography. *Proceedings of the National Academy of Sciences*, *84*(20), pp.7109-7113.

St-Jacques, B., Hammerschmidt, M. and McMahon, A.P., 1999. Indian hedgehog signaling regulates proliferation and differentiation of chondrocytes and is essential for bone formation. *Genes & Development*, *13* (16), pp. 2072-2086.

Trueta, J., 1963. The role of the vessels in osteogenesis. *J. Bone Joint Surg*, *45* (2), pp. 402-418.

Urist, M.R., 1965. Bone: formation by autoinduction. *Science*, *150* (3698), pp. 893-899.

Van Eeden S.P. and Ripamonti, U. 1994. Bone differentiation in porous hydroxyapatite in baboons is regulated by the geometry of the substratum: implications for reconstructive craniofacial surgery. *Plast Reconstr Surg*, *93*, pp 959-966.

Vlodavsky, I., Folkman, J., Sullivan, R., Fridman, R., Ishai-Michaeli, R., Sasse, J. and Klagsbrun, M., 1987. Endothelial cell-derived basic fibroblast growth factor: synthesis and deposition into subendothelial extracellular matrix. *Proceedings of the National Academy of Sciences*, *84*(8), pp.2292-2296.

Vu, T.H., Shipley, J.M., Bergers, G., Berger, J.E., Helms, J.A., Hanahan, D., Shapiro, S.D., Senior, R.M. and Werb, Z., 1998. MMP-9/gelatinase B is a key regulator of growth plate angiogenesis and apoptosis of hypertrophic chondrocytes. *Cell*, *93* (3), pp. 411-422.

Vukicevic, S., Luyten, F.P., Kleinman, H.K. and Reddi, A.H., 1990. Differentiation of canalicular cell processes in bone cells by basement membrane matrix components: regulation by discrete domains of laminin. *Cell*, *63* (2), pp. 437-445.

Wozney, J. M. *et al*., 1988. Novel regulators of bone formation*:* Molecular clones and activities. *Science, 24* (4885):1528-1534.

Wozney, J. M., 1992. The bone morphogenetic protein family and osteogenesis. *Wiley Subscription Services, Inc., A Wiley Company, 32* (2), pp.160-167.

Yuan, H., Van Den Doel, M., Li, S., Van Blitterswijk, C.A., De Groot, K. and De Bruijn, J.D., 2002. A comparison of the osteoinductive potential of two calcium phosphate ceramics

implanted intramuscularly in goats. *Journal of Materials Science: Materials in Medicine*, *13*(12), pp.1271-1275.

APPENDICES

Appendix A: Title Approval

UNIVERSITY OF THE
WITWATERSRAND,
JOHANNESBURG

Private Bag 3 Wits, 2050
Fax: 027117172119
Tel: 02711 7172076

Reference: Mrs Sandra Benn
E-mail: sandra.benn@wits.ac.za

06 January 2017
Person No: 1298238
PAG

Dr AB Alkonti
36 Burg Street
Namaqa House
Capetown
8001
South Africa

Dear Dr Alkonti

Master of Science in Dentistry: Approval of Title

We have pleasure in advising that your proposal entitled *Patterns of bone induction by coral-derived vs. highly sintered crystalline hydroxyapatite constructs* has been approved. Please note that any amendments to this title have to be endorsed by the Faculty's higher degrees committee and formally approved.

Yours sincerely

Mrs Sandra Benn
Faculty Registrar
Faculty of Health Sciences

Appendix B: Ethical Waiver

UNIVERSITY OF THE WITWATERSRAND, JOHANNESBURG
7 York Road, Parktown, 2193 South Africa * Telephone (011)717-2363

30 March 2016

To: Whom it may concern,

Re: Waiver from Animal Ethics Screening Committee

This letter is to confirm that Dr Assaedi Basher Alkonti (Student Number 1298238) is currently enrolled for postgraduate studies (MSc Dent in Oral Medicine & periodontology). He does not require full clearance from the Animal Ethics committee for the study titled "*Patterns of bone induction by coral-derived hydroxyapatites vs. highly sintered crystalline hydroxyapatite constructs*".

The study is supervised by Prof Ugo Ripamonti.

Dr Alkonti's study involves the retrospective analysis of decalcified and undecalcified histological sections already prepared and stored in the archives of the Bone Research Laboratory.
All the surgical procedures and tissue harvesting were conducted by Professor Ripamonti. Ethical clearance for the original studies was granted to Professor Ripamonti by the AESC.

Yours sincerely,

Kennedy Erlwanger
(Chairman: Animal Ethics Screening Committee, University of the Witwatersrand)

Reference Number: A.B Alkonti 30.03.2016-O

Assoc Prof Kennedy H. Erlwanger
School of Physiology
Faculty of Health Sciences, University of the Witwatersrand
7 York Road, Parktown, 2193
SOUTH AFRICA

Private bag 3, Wits, 2050, South Africa.
Tel: +27 (0)11 717 2454
Email: Kennedy.Erlwanger@wits.ac.za

Appendix C: Plagiarism Report

Dr

by Assaedi2 Alkonti2

Submission date: 02-Aug-2017 09:56AM (UTC+0200)
Submission ID: 834671591
File name: 02082017.docx (7.04M)
Word count: 9108
Character count: 68665

Dr

ORIGINALITY REPORT

11%	11%	14%	4%
SIMILARITY INDEX	INTERNET SOURCES	PUBLICATIONS	STUDENT PAPERS

MATCH ALL SOURCES (ONLY SELECTED SOURCE PRINTED)

11%

★

"Regenerative Medicine, the Induction of Bone Formation, Bone Tissue Engineering, and the Osteogenic Proteins of the Transforming Growth Factor-β Supergene Family", Induction of Bone Formation in Primates, 2015

Publication

Exclude quotes	On	Exclude matches	< 1%
Exclude bibliography	On		